AD NUMBER
AD913801
LIMITATION CHANGES

TO:

Approved for public release; distribution is unlimited.

FROM:

Distribution authorized to U.S. Gov't. agencies only; Test and Evaluation; JUN 1973. Other requests shall be referred to Office of Naval Research, Arlington, VA 22203.

AUTHORITY

ONR ltr 2 Mar 1979

AD913801

PSR REPORT 306

June 1973

ELECTROMAGNETIC COMMUNICATION IN THE EARTH'S CRUST

F.C. Field
M. Dore

PACIFIC·SIERRA RESEARCH CORP.

1456 Cloverfield Blvd. · Santa Monica, California 90404

PSR REPORT 306

June 1973

ELECTROMAGNETIC COMMUNICATION IN THE EARTH'S CRUST

E.C. Field
M. Dore

PACIFIC·SIERRA RESEARCH CORP.

1456 Cloverfield Blvd. · Santa Monica, California 90404

ARPA Order No.: ● 2770

Program Code No.: 3F10

Name of Contractor: Pacific-Sierra Research Corp.

Effective Date of Contract: 72 November 01

Contract Expiration Date: 73 December 31

Amount of Contract: $68,010.00

Contract Number: N00014-73-C-0189

Principal Investigator: Edward C. Field

Scientific Officer: John G. Heacock

Phone Number: (213) 828-7461

Short Title of Work: Lithospheric Communication

PREFACE

Pacific-Sierra is performing a study of possible military applications for an electromagnetic waveguide in the lithosphere. This report presents the results of the first phase of that study; viz., a determination of the data rates and transmission ranges that, based on currently used models of the lithosphere, might be achievable with reasonable power expenditure and antenna burial depths. These results form the scientific basis for the second phase of the study, which is to determine those missions for which use of a lithospheric communication link could be feasible.

The motivation for this work stems from the integrated studies of crustal properties that have been conducted for a number of years by the Earth Physics Program of the Office of Naval Research. This effort was brought into focus by a Symposium, jointly sponsored by ONR and CIRES, held in July 1970. The proceedings of this symposium were published in AGU Monograph #14, *The Structure and Physical Properties of the Earth's Crust (1971)*. Subsequently, two workshops, funded by ARPA and organized by ONR, were held at the Colorado School of Mines, in February 1972, to define an experimental program to ascertain the existence of the lithospheric waveguide.

SUMMARY AND CONCLUSIONS

This report presents results of an analysis of the capabilities
that might be achieved with a lithospheric communication system. The
analysis uses several available models of continental lithospheric
conductivity as inputs to calculations of transmission characteristics
and possible communication system parameters. Because of prevailing
uncertainties, significant differences exist among the various models;
and a wide range of future system capabilities is found to lie within
the realm of possibility. Full-wave modal solutions that take full
account of vertical conductivity gradients are used to calculate attenua-
tion rates, field-strength depth-profiles, and transfer functions
relating the noise fields at depth to those measured at the surface.
Also, estimated values of required system power are given as a function
of data rate, transmission range, and receiver burial depth. Carrier
frequencies from 100 Hz to 100 kHz are considered. It could well prove
worthwhile, however, to extend the analysis to frequencies outside of
the ELF/VLF/LF bands treated herein.

For all models used, the calculated attenuation rates are con-
siderably larger than for above-ground transmission, which depends on
propagation in the earth-ionosphere waveguide. In spite of this fact,
reasonably large transmission ranges might be possible in the lithosphere
because the atmospheric noise fields at depth are very small, having
suffered heavy attenuation in propagating downward from the earth's
surface.

The major factor affecting system feasibility is whether water-
saturated microcracks exist in all major rock types at depths greater

than, say, 5-to-8 km. If such microcracks exist (as assumed in one model), and minimum conductivities in the crust exceed 10^{-5} - 10^{-6} mhos/m, then the calculations show clearly that a practical communication system is not feasible. For this case, the attenuation rates are so high that only very short transmission ranges could be achieved, even if large amounts of power were expended. Field experiments will be needed to determine with certainty whether saturated microcracks are, in fact, present at the depths of interest. However, valid reasons exist for optimism that fluids (or fluid films) should not be an important factor at depths greater than several kilometers, and that conductivity profiles (at depth) based on laboratory data for dry rocks more closely approximate actual conditions. Further, recent laboratory data indicate that the conductivity of dry rock in the crust could be much lower (10^{-8} to 10^{-9} mhos/m) than previously believed (10^{-7} mhos/m). It is, of course, difficult to relate data obtained from laboratory samples to conductivities of rock *in situ*. Nonetheless, calculations using conceptual profiles based on the assumption of dry basement rock yield results that are quite encouraging. For example, for data rates of a few tens of bits-per-second and power expenditures of 1-to-10 megawatts, transmission ranges of from about 1000 to many thousands of kilometers (depending on the profile used) appear to be a possibility.

The calculations show clearly that much larger transmission ranges can be achieved in the LF band (30-100 kHz) than at the lower frequencies considered. This effect is due mainly to the heavy attenuation suffered by downward propagating atmospheric noise at the higher frequencies. The calculations also show that the maximum transmission

ranges are somewhat sensitive to the details of the model profiles.
For example, for two profiles exhibiting the same minimum conductivity,
the transmission range (for a specified power, etc.) can vary by a
factor of two depending on the conductivity depth-gradients, and the
precise location of any sharp transition layers that might exist.

The depth to which a receiver must be buried to achieve satisfac-
tory performance is a particularly important parameter, since borehole
drilling costs could be a large fraction of the total system cost.
The transmission ranges given above apply when the receiving antenna
is located near the "center" of the waveguide--assumed to be about
ten kilometers deep for the conductivity profiles used in this
report. For profiles representative of regions stripped of highly
conductive sedimentary layers, the calculations show that receiver
depths as shallow as 3 or 4 km could be used at only a 15-to-20 percent
penalty in transmission range. One implication of this fact is that--
previous negative results notwithstanding--a meaningful propagation
experiment could be carried out with relatively shallow boreholes,
provided that the region was carefully selected. Frequencies of
several tens of kilohertz would be preferable, and care should be
taken to insure a reasonable transmitter efficiency. Of course,
deeper boreholes would be needed in regions having thick, highly
conducting overburdens.

Another type of propagation experiment, not involving a trans-
mitter, has appeal for ascertaining the existence, or non-existence,
of a lithospheric waveguide. There are regions of the sea floor where
little or no sedimentation exists, and where energy propagating in a

lithospheric waveguide could conceivably approach the ocean's bottom from below. In deep water, the preferred propagation path (to the bottom) for atmospheric noise would be via a lithospheric duct, rather than downward from the ocean's surface, due to the opacity of sea water to all frequencies higher than, say, a few Hertz. Consider an experiment where atmospheric noise was measured as a function of the depth (in the water) of the receiving antenna. For shallow receiver depths, this noise would decrease as the receiver depth was increased. If, however, the noise (e.g., Schumann resonances) was then found to increase as the receiver approached or contacted the bottom, considerable credence would be given to the presumed existence of a crustal waveguide.

CONTENTS

I. INTRODUCTION

More than a decade has passed since the existence of an electro-
magnetic waveguide in the earth's crust was first postulated (e.g.,
Wait, 1954; Wheeler, 1961). The assumption was that conductive, wet
surface layers and conductive, hot mantle layers enclose a resistive
zone of dry basement rocks. As originally conceived, the resistive
zone occupied depths between roughly 10 and 30 km. Interest in ascer-
taining the existence, or non-existence, of this lithospheric waveguide
stemmed from its potential use as a communication channel. In the
intervening years enthusiasm about the prospect of a crustal waveguide
waned, partially because of the apparently negative outcome of propaga-
tion experiments carried out between 1962 and 1966 (....., ...).
In retrospect, it appears that, due to experimental limitations, the
data thus obtained could not have either confirmed or denied the exis-
tence of a waveguide in the lithosphere.

Little is known in detail about the precise nature of the materials
and physical properties of the earth's crust at depths where the resistive
basement rocks are presumed to exist. The available data base is by
no means complete, and additional field measurements are needed if firm
values are to be assigned to key parameters. However, reinterpretation
of available field data has indicated that conductivities of 10^{-7} mhos/m
or lower could exist. Moreover, recent laboratory experiments on the
conductivity of dry rock, and recent evidence based on minerological
considerations, suggest cause for optimism that conductivities lower
than previously believed might exist in the crust (e.g., $\leq 10^{-8}$ mhos/m).
Theoretical analyses show that the corresponding attenuation rates for

electromagnetic waves could be low enough to permit communication over useful distances. For these reasons, there has been renewed interest in determining the electrical properties of the lithosphere and in assessing its potential utility as a communication channel. Workshops have been held, and recommendations made that interdisciplinary field-measurement programs be undertaken (*Keller, 1974; Hales, 1972*).

This report presents results of an analysis of capabilities that might be achieved with a lithospheric communication system. As might be expected in view of prevailing uncertainties, a wide range of future system capabilities is found to lie within the realm of possibility. However, the results give guidance as to whether it is reasonable to expect, on the basis of current knowledge, that a lithospheric wave-guide would provide the basis for useful communication links.

The lithospheric conductivity models used in the calculations are given and discussed in Sec. II, as are models of atmospheric and thermal noise. The mathematical methods used are described in Sec. III, and numerical results, obtained from Pacific-Sierra's long-wave propagation code are given in Sec. IV.

II. MODELS OF ELECTRICAL CONDUCTIVITY AND NOISE IN THE LITHOSPHERE

The electromagnetic transmission properties of the lithosphere must be calculated in order to assess its utility as a communication channel. This calculation requires a knowledge of the depth-profiles of the electrical properties (primarily conductivity) of the earth's crust and upper mantle, as well as a knowledge of the degree of lateral homoegneity of these properties. In addition, tl noise environment at the receiver must be known to determine the relationships among radiated power, transmission range, and data rate. Accordingly, the models of conductivity and noise spectrum used as inputs to the calculations of Secs. III and IV are discussed below.

CONDUCTIVITY DEPTH-PROFILES

Considerable uncertainty exists as to the conductivity of the earth at depths greater than several kilometers. This uncertainty is due to practical difficulties encountered in using surface-based sounding techniques to detect low conductivities at depth, and an absence of sufficiently deep boreholes for direct measurements. However, nominal models for conductivity depth-profiles in the lithosphere have been suggested by various geophysicists. As might be expected in view of the prevailing uncertainties, significant differences exist among currently available model profiles. This state of affairs is unfortunate, since the results given in Sec. IV show that the transmission properties of the lithosphere depend strongly on the minimum value of conductivity in the crust, as well as on the depth-gradients of the conductivity.

It is necessarily beyond the scope of this study to determine the correct depth-profile of conductivity in the lithosphere. Indeed, the main goal of the *Crustal Studies Workshop (Hales, et al., 1972)* was to consider and suggest experimental procedures by which profiles could be determined. The approach taken in this report is to use currently available conductivity profiles, which in our opinion are reasonable in the context of present knowledge, as inputs to our calculations. This approach provides the most reliable estimates that can now be made of the expected performance of a lithospheric communication system, and also indicates the sensitivity of lithospheric transmission properties to variations in the profiles. Guidance is thereby obtained as to whether more extensive experimental determinations of lithospheric conductivities are likely to reveal the existence of a useful crustal waveguide.

For a discussion of evidence for (and against) the existence of an electromagnetic waveguide in the lithosphere, the reader is referred to *AGU Monograph 14 (Heacock, ed., 1971)* and *Crustal Studies Workshop Report (Hales, 1972)*. Briefly, the conductivity of rocks near the earth's surface is relatively high due to the presence of water in pores and cracks. As the depth is increased, the contribution of pores and cracks to the conductivity is diminished due to increasing pressure; the conductivity will therefore decrease with increasing depth. There is, however, a competing effect; viz., the temperature increases by some 10°-to-30°K for each additional kilometer of depth. Ultimately, conductivity due to thermal-activated carriers in hot rock should become dominant. The conductivity should then increase with increasing

depth. There is thus reason to expect a layer of relatively low
conductivity to exist between a surface layer (overburden) that is
highly conductive because it contains fluid and a sub-basement that
is highly conductive because it is hot. This poorly conducting layer,
if it exists, would comprise the lithospheric waveguide that is the
subject of this study. Geophysicists have given much attention to
ascertaining the minimum value of conductivity in the waveguide, since
this value strongly influences the transmission properties. Presently,
the value of minimum conductivity is uncertain by several orders of
magnitude.

For the purpose of making calculations, the so-called "step-
function" representation of the conductivity profile is the simplest.
Here, the lithosphere is assumed to form a uniform parallel-plate
waveguide, bounded on the top by a highly conducting overburden and on
the bottom by a highly conducting sub-basement. The region between
these two sharp boundaries contains rock of low conductivity. *Spies
and Wait (1971)* performed an extensive and useful parametric study of
the transmission properties of a parallel-plate model of the lithosphere.
Specifically, they calculated attenuation rates and excitation functions
as functions of wave frequency, waveguide width, waveguide conductivity,
and boundary conductivity. Although the step-function representation
of the conductivity profile provides insight into the dependence of the
transmission on several key parameters, we have chosen to use more
detailed profiles. This choice was made because 1) the signal attenua-
tion depends on the depth-gradients of the conductivity, which cannot
be included in a step-function profile; and 2) the depth to which

antennas must be buried to provide adequate reception (or radiation) cannot be calculated satisfactorily from a step-function model. To ascertain the depth dependences of the signal and noise fields, finite conductivity gradients must be included in the model.

A major source of uncertainty is the water content of rocks at depths greater than a few kilometers. One view holds that microfractures are not present in rocks at depths that have never been mechanically unloaded from lithostatic compression. Such rocks would be dry and have a very low electrical conductivity. Another view is that water films in microcracks must be present at all depths in the crust[*] (*Brace, 1971*). Hypothetical conductivity profiles that illustrate the implications of the above two points of view have been prepared by *Levin (1971)* and are shown in Fig. 1. Each profile exhibits a "waveguide" at depths between about 10 and 30 km. The conductivities at shallow depths are based upon available, shallow geophysical measurements; those below about 30 km are estimated from assumed temperature gradients in the rock. The profiles shown in Fig. 1 differ only in the "waveguide" region between 10 and 30 km. The segments labeled "wet" and "dry" are nominal representations based upon early laboratory measurements of "wet" and "dry" rocks, respectively. Under the hypothesis of "wet" rock, the minimum conductivity shown is about 10^{-5} mhos/m; and for dry rock, about 10^{-7} mhos/m. The profiles in Fig. 1 are intended only to illustrate the range of uncertainty in the expected minimum conductivity, and are nominal rather than detailed

---

[*] Whether such saturated microcracks exist in all major rock types *in situ* is still undetermined. However, for several reasons, there appears to be increasing optimism that dry, low-conductivity zones can exist in the crust (see, e.g., *Hales, 1972*; p. 28).
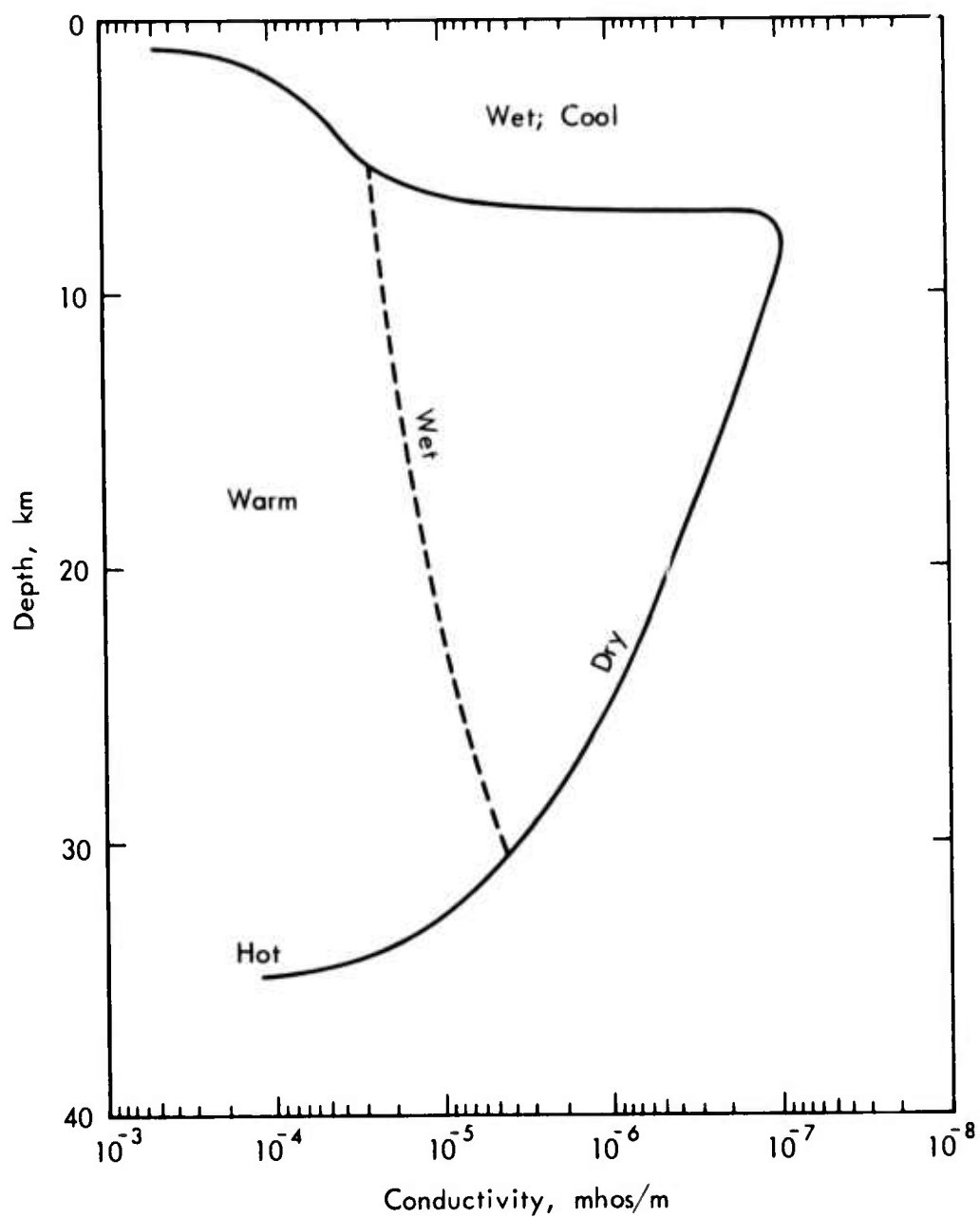
Fig. 1--Conductivity Profiles of the Crust According to
Two Hypotheses (after *Levin, 1971*)

representations. Further, as discussed below, recent laboratory measurements—not available when Levin's profiles were prepared—indicate that the minimum conductivity could well be considerably less than 10^{-7} mhos/m.

Of the currently available conductivity profiles, the one based on the most extensive measurements is probably that shown in Fig. 2 (*Keller* as reported by *Gallawa and Haidle, 1972*). Although uncertain in several respects, this profile represents a compilation of a good deal of geophysical and laboratory data. The conductivities shown for relatively shallow depths are based upon well-log data, taken in Appalachia, that clearly indicate a decreasing conductivity down to at least several kilometers. This decreasing trend in conductivity is believed to be controlled by the rate at which fractures close due to increasing overburden pressure. Below, say, 3-to-5 km, the decrease in conductivity was extrapolated, in a manner consistent with available field and laboratory data, to a minimum value referred from recent field measurements.[*] Below about 10-to-12 km, the conductivity is assumed to be dominated by high-temperature mineral conduction. The values shown for depths below 10-to-12 km in Fig. 2 are based on laboratory measurements of high-temperature rocks. The assumed temperature scale is shown on the right-hand axis of Fig. 2, and corresponds to a nominal thermal gradient of 16°/km.

In addition to temperature, the conductivity at depth also depends on mineralogy. Note that in Fig. 2 Keller has assumed a rapid transition

---

[*] For a discussion of the various methods of probing the electrical properties of the crust, and a discussion of the difficulty in obtaining and interpreting data on deep layers of low conductivity, see *Keller (1971)*.
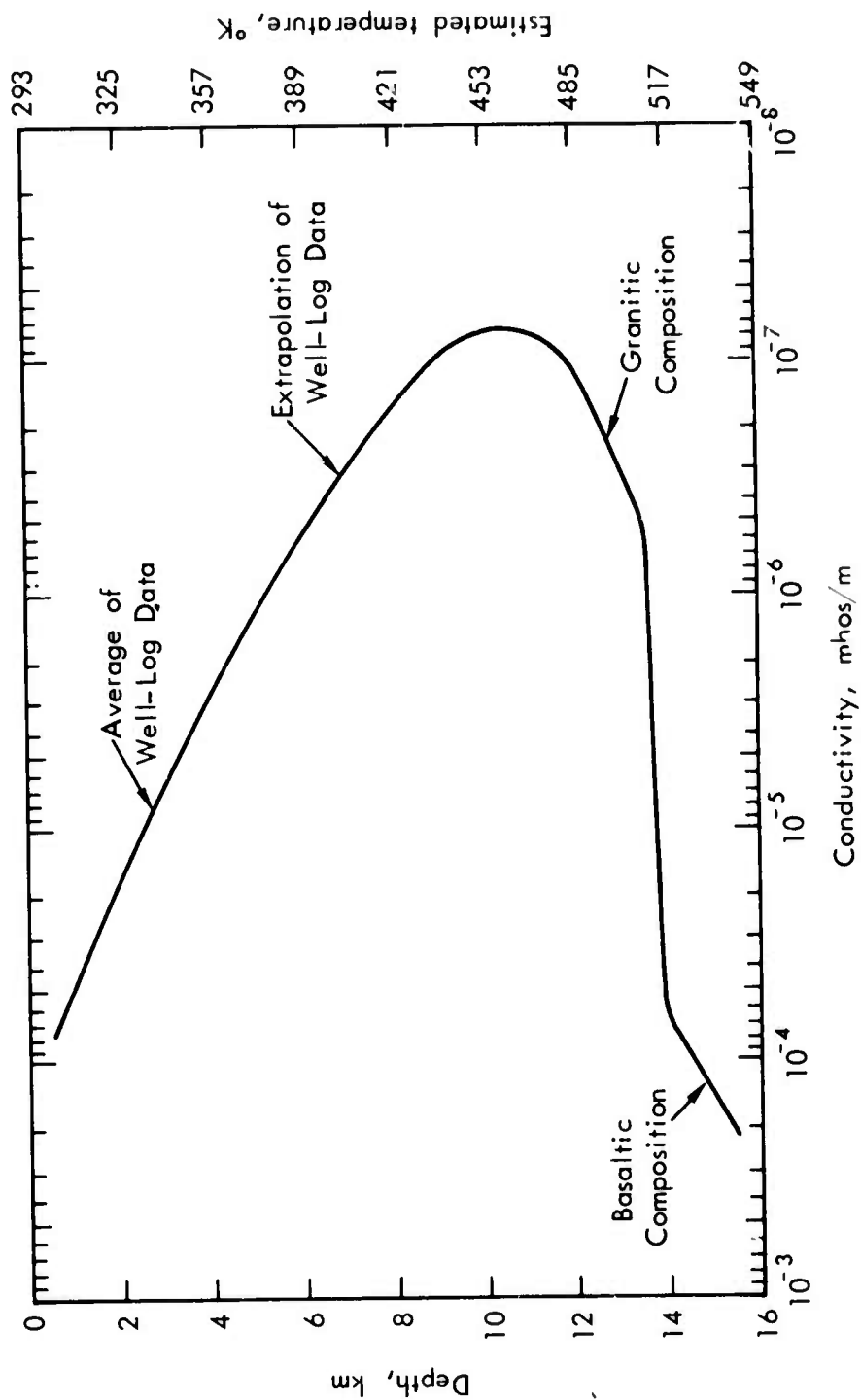
Fig. 2—Conductivity and Temperature Profile in the Crust (after Keller, as reported by Gough and Haidle, 1972)

in conductivity at about 14 km. The existence of such a transition is inferred from seismic data and certain electromagnetic field measurements. The 14-km depth at which the transition is assumed to occur is, of course, nominal, and represents an average value for the United States. In some regions, assumed transition-layer depths as large as 20-to-25 km are consistent with the available data *(Keller, 1973)*. Another characteristic of the Keller profile is that the conductivity at the earth's surface is taken to be about 10^{-4} mhos/m--a very low value. The use of a higher surface conductivity (say, 10^{-2} to 10^{-3} mhos/m) would not change the conclusions of this report significantly, since the transmission properties of the waveguide depend mainly on the properties of the crust at depths below 1 or 2 km.

Recent laboratory measurements of the conductivity of dry rock reported by *Housley (1973)* suggest that the minimum conductivity of the crust might be considerably less than illustrated in Figs. 1 and 2. He argues that most previous laboratory data tend to give a misleading picture of lithospheric conductivity at depths greater than, say, 10 km. Rocks *in situ* should have much lower conductivity than rocks that have been exposed to the atmosphere and that have had microcracks closed by the application of high pressures in the laboratory. In the latter case, thin films of interstitial fluid remain and raise the conductivity by a considerable amount. In addition, Housley has found that the partial pressure of oxygen in the atmosphere surrounding the sample must be maintained at a level corresponding to that in the crystal at the temperature and pressure for the depth being simulated. The data thus obtained indicate conductivities orders of magnitude less

than previously measured for dry rocks in the laboratory. If one uses these new conductivity data, and follows the same reasoning (see above) that led to the profile shown in Fig. 2, the resultant profiles are as shown in Fig. 3. These profiles are identical to Keller's (Fig. 2) for depths less than about 10 km, since the same data and assumptions are used. At greater depths, however, much lower conductivities ($<10^{-8}$ mhos/m) are indicated, due to the new laboratory data described above. The three profiles shown correspond to geotherms in three different heat-flow provinces,[*] as reported by *Blackwell (1971)*. The thermal gradients used were BR ($\sim 24°$/km), EUS ($\sim 14°$/km), and SN ($\sim 9°$/km) as compared with the 16°/km used for the Keller profile (Fig. 2).

It must be emphasized that the Fig. 3 profiles (or any others) are by no means definitive, and much experimental work remains (some of which is now underway) before a satisfactory understanding of the conductivity of *in situ* rocks can be attained. Great uncertainty is involved in using laboratory data to infer the conductivity of the crust. Further, the data reported by *Housley (1973)* were for only a single sample (olivine); but lithologies are not constant in nature. However, these data do give encouragement that the minimum conductivity of the crust might be lower than previously believed.

Clearly, the above discussion indicates selecting a single "best" profile for making calculations would be impossible. Indeed, Fig. 3 alone shows the large variations that would occur among different provinces. The Levin profile (Fig. 1) exhibits rather abrupt changes in conductivity at depths of about 2 km and 7 km. The Keller profile

---

[*] BR (Basin and Range), EUS (Eastern, US), SN (Sierra Nevada).
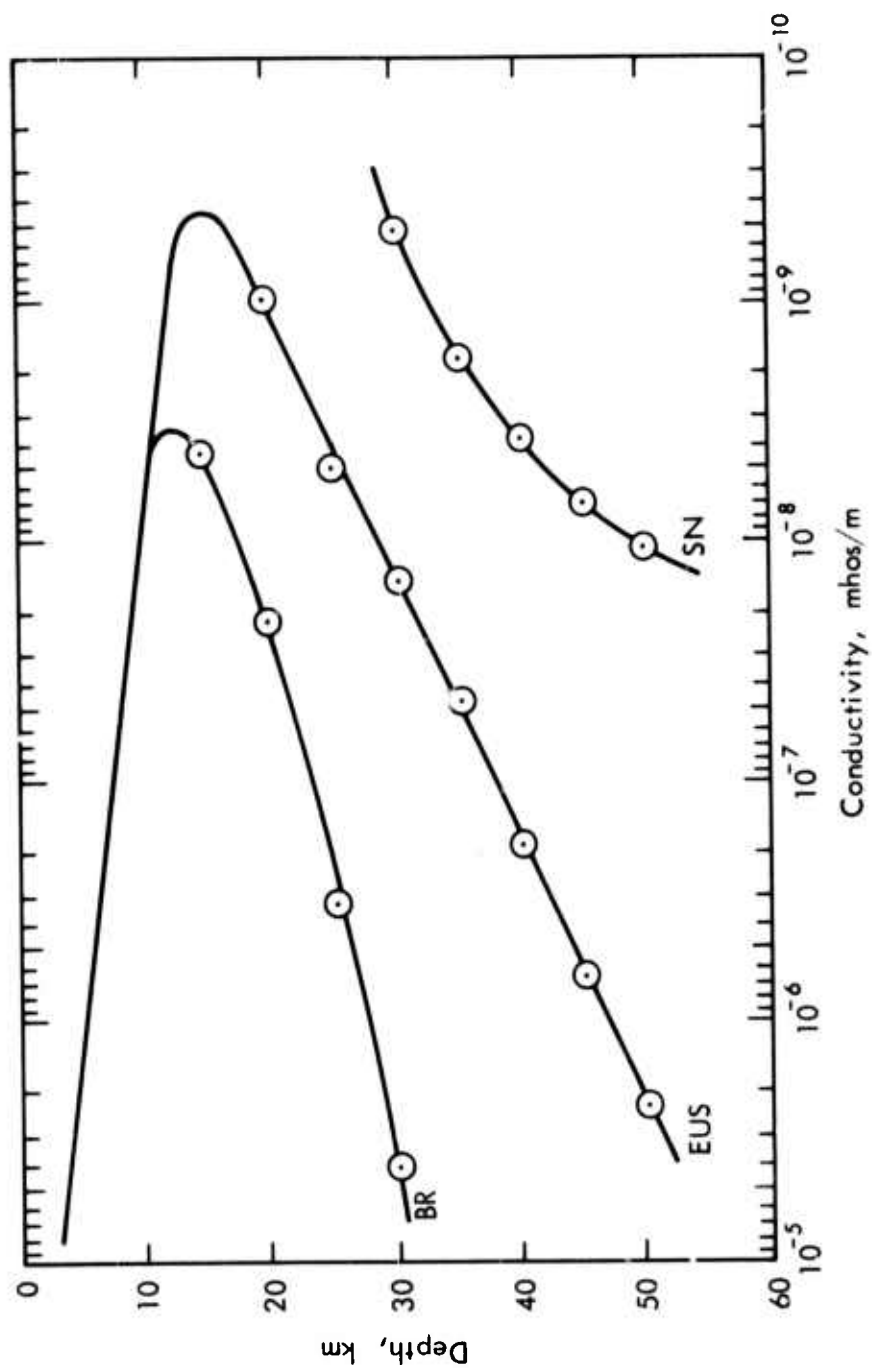
Fig. 3—Conductivity Profiles in the Crust for Three Heat-Flow Provinces (after *Housley, 1973*)

(Fig. 2) exhibits a near-discontinuity at around 14 km; whereas the
Housley profiles (Fig. 3) are quite smooth at all depths.[*] Field
measurements are needed to determine which of the differences between
these (and other) profiles are artificial, and which correctly account
for real differences among various regions of the earth's crust. It
would not be practical, or very meaningful, to undertake detailed trans-
mission calculations for *all* available conceptual profiles. In Sec. IV,
rather complete computational results are given for the Keller and
Housley BR profiles; and sample results for other profiles, to indicate
important trends. When more accurate conductivity measurements become
available, the methodology developed here can be applied to obtain
more reliable estimates of the transmission properties.

ATMOSPHERIC AND THERMAL NOISE

The noise environment at a buried receiver consists of thermal
noise, which depends upon the temperature distribution in the crust, and
atmospheric noise, which propagates downward from the earth's surface.
We use the temperature profile given in Fig. 2 to compute thermal noise.
As discussed in Sec. III, reasonable variations from this profile change
the thermal-noise power density at the receiver by an insignificant
amount.

Extensive data for atmospheric noise at the earth's surface are
available for various seasons and geographic locations. We use data

---

[*]As shown in Sec. IV, the transmission properties of the litho-
sphere depend strongly on whether abrupt transitions in the conductivity
profile are present. In fact, some of the calculations given below are
for the Housley BR profile, modified to have a sharp transition at a
depth of 25 km.

compiled by *Maxwell (1967)*. His rms noise-density spectra for summer

and four representative locations are shown in Fig. 4. Maxwell's data

indicate that these rms atmospheric noise values are exceeded 10-to-20

percent of the time. Thus, a system designed on the basis of the rms

atmospheric noise will achieve, or exceed, performance specifications

80-to-90 percent of the time; i.e., it will have an 80-to-90 percent

time availability. If 99-percent time availability is required, then

the system should be designed on the basis of atmospheric-noise spectral

densities about 10 dB larger than those shown in Fig. 4. At the earth's

surface, the electric fields associated with atmospheric noise in the

ELF/VLF/LF bands are nearly vertical; whereas the magnetic fields are

nearly horizontal. The noise-field components at depth must be computed

for each conductivity profile from the surface-noise data. The details
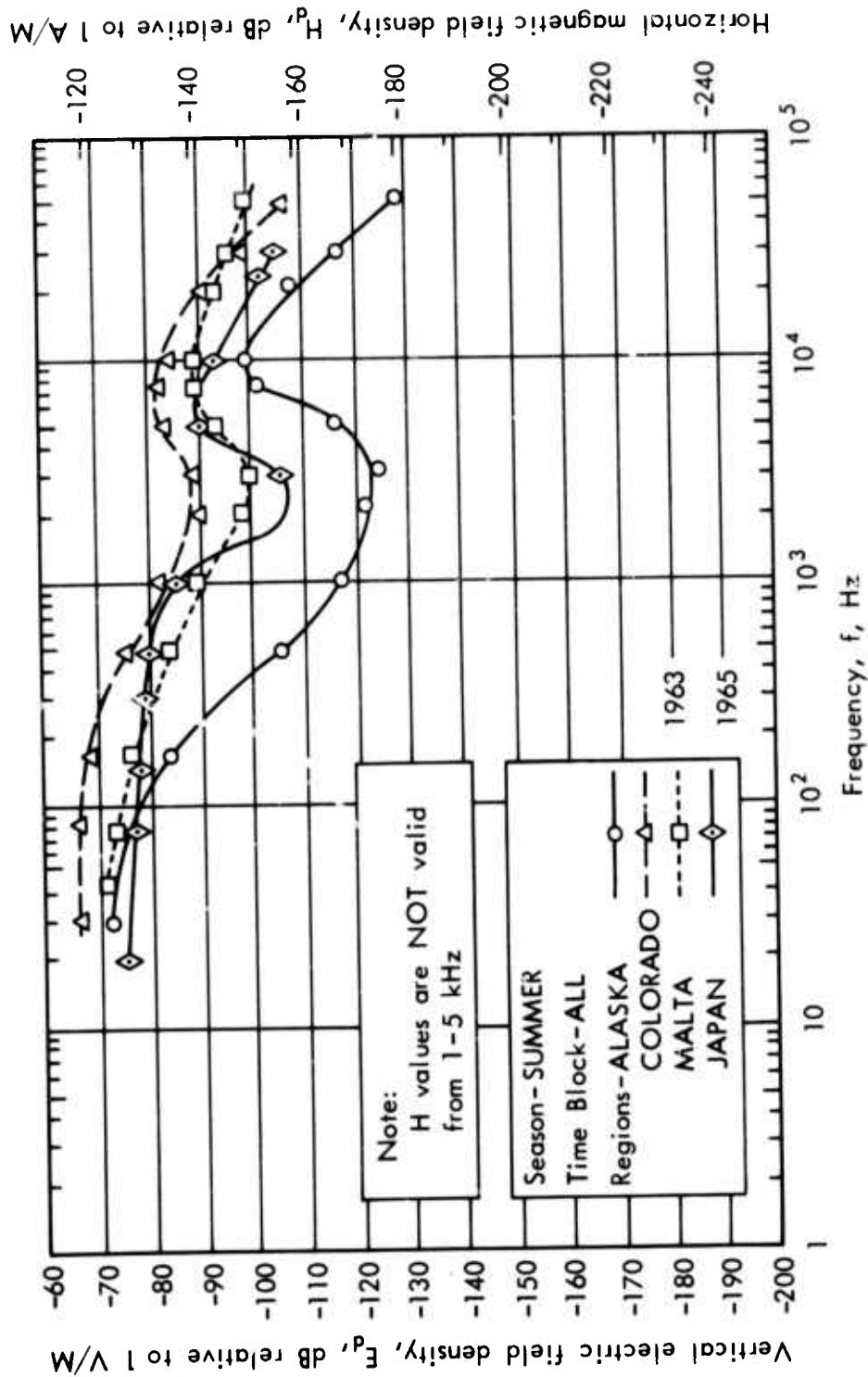
of this calculation are given in Sec. III.

Fig. 4—Geographic Dependency of Mean Noise-Density Spectra (after Maxwell, 1967)

III. MATHEMATICAL FORMULATION

In view of the inherent uncertainty in the conductivity depth-profiles given in Sec. II, the choice of computational method requires discussion. It is tempting to argue that highly simplified analytic techniques will suffice, since--regardless of the mathematical approach--the final results will be no more accurate than the models used for inputs. Although clearly correct, this argument should not be carried too far, lest important general characteristics of the electromagnetic fields be obscured. In particular, account must be taken of the depth gradients of conductivity to gain insight into the depth dependence of the signal and atmospheric noise fields. This insight is needed to determine the dependence of system performance on antenna burial depths. Clearly, if either transmitting or receiving antennas could be placed at relatively shallow depths above the waveguide, system costs would be reduced significantly. Conductivity gradients also strongly affect the lateral attenuation in the waveguide. Since the wavelengths involved are not small compared with vertical distances over which the electrical properties of the lithosphere change substantially, eikonal methods are not applicable and full-wave calculations are needed. To compute the lateral attenuation and depth dependence of the fields, we have used a method that accounts in detail for the vertical inhomogeniety of the lithospheric conductivity. We use simpler computational methods to account for lateral inhomogenieties and to determine certain system performance parameters.

MODAL SOLUTIONS

We wish to determine the spatial dependence of the electromagnetic fields propagating in a waveguide that is strongly inhomogeneous in the

vertical direction. The curvature of the earth will be neglected and horizontal stratification will be assumed (see Fig. 5). The method of calculation is a version of the waveguide mode analysis described by *Budden (1961)*. This method, often used in problems involving propagation in the earth-ionosphere waveguide (*e.g.*, *Field, 1970)*, has been modified in this study for application to the lithosphere.

Although the best antenna configuration for use in a lithospheric communication channel is not known, a vertically polarized E-field antenna is a likely candidate. We thus consider plane TM waveguide modes propagating in the x-direction, for which the electric field, E, and the magnetic field can be written

$$\underline{E}(x,z) = \left[\hat{e}_x E_x(z) + \hat{e}_z E_z(z)\right] e^{i(\omega t - k n_o S_o x)}, \tag{1}$$

$$\underline{\mathcal{H}}(x,z) = \hat{e}_y \mathcal{H}_y(z) \, e^{i(\omega t - k n_o S_o x)}.$$

In Eq. (1), $\mathcal{H} = \sqrt{\mu_o/\epsilon_o}\, H$, where H is the usual magnetic intensity, μ_o and ϵ_o are the electric and magnetic permittivities of free space, $\omega = 2\pi f$ (where f is the wave frequency), t is time, and $k = \omega/c$ (where c is the vacuum speed of light). MKS units will be used. The refractive index, n, is given by

$$n^2(z) = \epsilon(z) - \frac{i\sigma(z)}{\omega \epsilon_o}, \tag{2}$$

where σ is the depth-dependent conductivity and ϵ is the relative electric permittivity. The quantity n_o in Eq. (1) is the refractive index at the
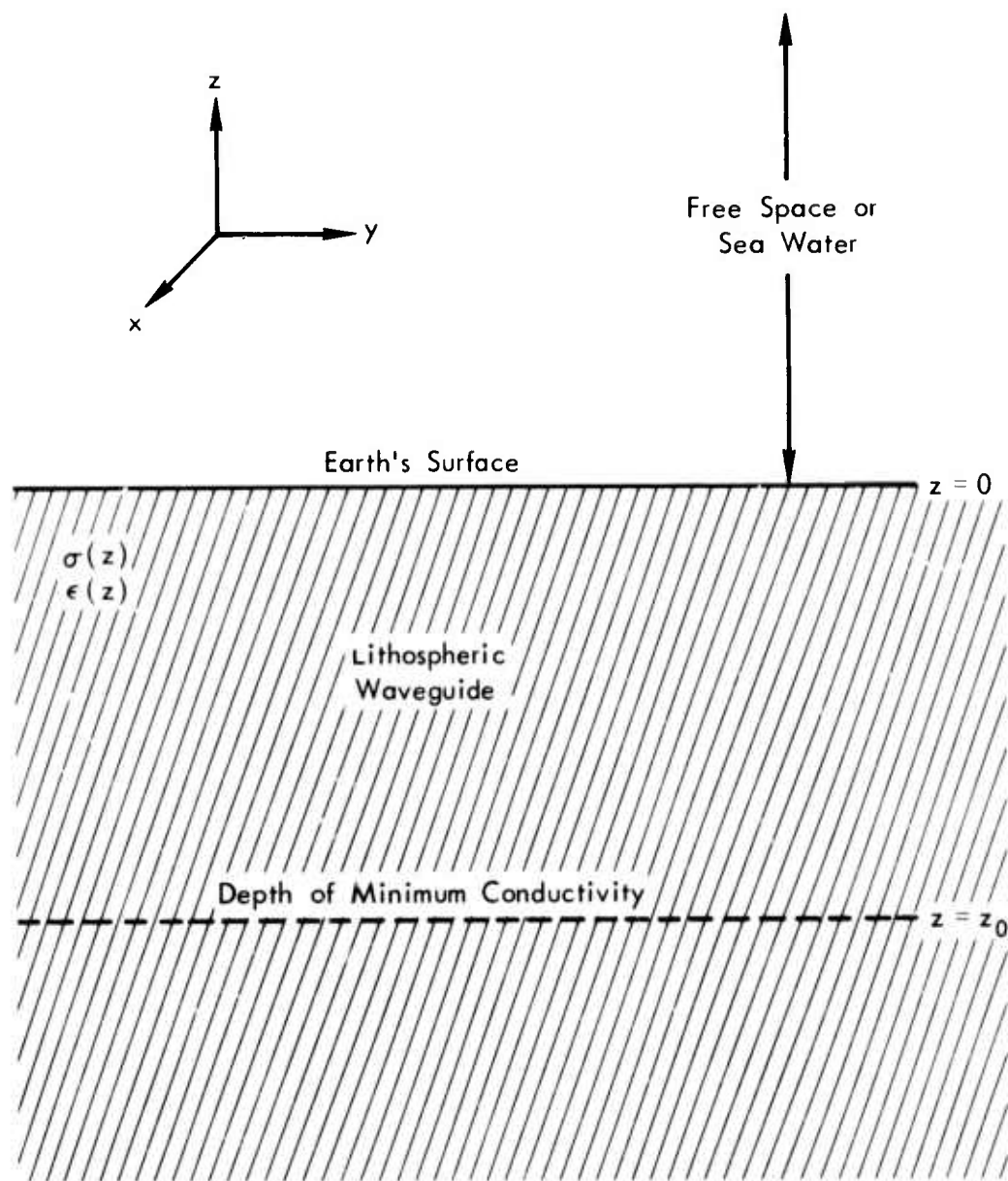
Fig. 5--Schematic Model of Lithospheric Waveguide

depth, z_o, of minimum conductivity in the lithosphere. S_o can be interpreted as the sine of the incidence angle at the depth z_o. Incidence angles at depths other than z_o can be determined from the relation

$$S(z)n(z) = n_o S_o = \text{constant}, \tag{3}$$

which follows from the assumed horizontal stratification and is essentially Snell's law.

The relevant Maxwell equations are:

$$\frac{dE_x}{dz} + ikn_o S_o \mathbb{1} = -ik\mathcal{H}_y ; \tag{4}$$

$$\frac{d\mathcal{H}_y}{dz} = -ikn^2(z)E_x ; \tag{5}$$

$$E_z = -\frac{n_o S_o}{n^2(z)} \mathcal{H}_y . \tag{6}$$

Rather than solving Eqs. (4) through (6) directly, we use the wave admittance, A, defined by

$$A \equiv \mathcal{H}_y/E_x , \tag{7}$$

and the related quantity

$$W = \frac{A-1}{A+1} . \tag{8}$$

By combining Eqs. (4) through (8), it follows that

$$\frac{dW}{dz} = -\frac{ik}{2}\left[n^2(z)(W-1)^2 - \left(\frac{n^2(z)-n_o^2 S_o^2}{n^2(z)}\right)(W+1)^2\right].\qquad(9)$$

It is clear from Eq. (1) that the lateral attenuation in the waveguide is governed by the product $n_o S_o$. Since n_o is specified once a lithospheric model and a wave frequency have been selected, only S_o must be calculated to determine the attenuation. This calculation involves the solution of Eq. (9) subject to the appropriate boundary conditions, whence eigenvalues for S_o are found. A guided wave in the lithosphere can produce only upgoing waves in the medium above the earth's surface, since this medium is assumed uniform with constant index of refraction, n_1. Thus, immediately above the earth's surface, the wave admittance is given by

$$A(0^+) = \frac{n_1^2}{[n_1^2 - S^2(0^+)]^{1/2}}.\qquad(10)$$

For propagation under the ocean, n_1 is the refractive index of sea water, and may be assumed infinite for the frequencies to be considered. For this case, $A(0^+) \to \infty$ and, from Eq. (8), the boundary condition for W is simply

$$W(S_{oN}, z=0) = 1,\qquad(11a)$$

where S_{oN} denotes the eigenvalue of S_o for the Nth mode. For the case where the medium above the earth's surface is free space, $n_1 = 1$; and, using Eqs. (3), (8), and (10), the boundary condition on W becomes

$$W(S_{oN}, z=0) = \frac{1-(1-n_o^2 S_{oN}^2)^{1/2}}{1+(1+n_o^2 S_{oN}^2)^{1/2}}.\qquad(11b)$$

The conductivity profiles given in Sec. II, and values for ϵ given below, are sufficient to determine $n^2(z)$ for the various models. Once n^2 is specified, Eqs. (9) and (11) comprise a closed set for W and S_{oN}. These coupled equations are solved readily by straightforward iteration. Each iteration requires the numerical solution of Eq. (9). This solution is started at a great depth, where a purely downgoing wave is assumed as an initial condition. In each solution, several starting depths and integration step sizes are tried; and the process is truncated when successive trials fall within a prescribed tolerance. The integration is terminated at the earth's surface. For a profile such as that shown in Fig. 2, it is inconvenient numerically to use downgoing waves at great depths as an initial condition, since integration across any zones of rapid conductivity change (which, for the case shown in Fig. 2, would be at 14 km) would be required on each iteration. For the profile in Fig. 2, we found that the use of $W(z=-14) = 1$ as an initial condition provided good accuracy and considerable simplification. This initial condition is equivalent to truncating the conductivity profile in a perfect conductor at $z=-14$ km.

Once the eigenvalue S_{oN} is found and W (and hence A) is computed, the attenuation rate for the Nth mode and the depth dependence of the electromagnetic fields are easily obtained. The attenuation rate is given by

$$\alpha_N = 8.7 \times 10^3 k \, \mathrm{Im} S_{oN} \qquad \mathrm{dB/km} \; ; \qquad (12)$$

and, by integrating Maxwell's equations, it follows that

$$\mathscr{N}_y(z) = \exp\left[-ik \int_{z_o}^{z} dz' \, \frac{n^2(z')}{A(z)} \right] , \qquad (13)$$

$$E_z(z) = -\frac{n_o S_o}{n^2(z)} \mathcal{X}_y(z),$$ (14)

and

$$E_x(z) = \mathcal{X}_y(z)/A(z),$$ (15)

where $\mathcal{X}_y$ has been taken to equal unity at the "center" of the waveguide; i.e., at $z = z_o$. The time and x-dependence of the fields have been suppressed in Eqs. (13) through (15).

ATMOSPHERIC AND THERMAL NOISE

To calculate achievable transmission ranges and data rates in the lithosphere, it is necessary to know the atmospheric and thermal-noise spectral density at the receiver depth. The atmospheric noise fields at depth must be calculated from the available data, which are typically in the form of vertical electric fields measured at the earth's surface (see Fig. 4). The quantities that relate the noise fields at depth to the surface noise fields will be called noise-transfer functions. For uniform media, such as the ocean, the transfer functions can be calculated easily in terms of plane waves and the well-known Fresnel reflection and transmission coefficients. However, when the conductivity exhibits significant depth-gradients (e.g., as in Figs. 1-3), the transfer functions cannot be computed in closed form. *Gallawa and Waidle (1972)* accounted for the vertical inhomogeniety of conductivity by representing the lithosphere by several uniform layers and computing the transfer function by summing the absorptions suffered in each layer. However, even this approach is not adequate for the problem at hand. It neglects both the

conversion loss suffered at the earth's surface and the fact that the admittance "seen" by a downward propagating signal involves an integral over all depths. Also, the total noise field at depth should not be used. Instead, the component of the noise field in the direction of the antenna polarization is needed. Although the noise fields above the earth's surface are nearly vertically polarized, the fields in the highly refractive earth can be nearly horizontally polarized. And a vertically-oriented, buried electric antenna (a likely configuration) will be less sensitive to atmospheric noise than would a horizontally oriented one. In fact, the strength and polarization of the subterranean noise fields are related in a complicated fashion to the conductivity profile and change continuously with depth. A full-wave numerical calculation of these fields is thus needed. Fortunately, the procedures developed to solve Eqs. (9) and (13) through (15) can be used essentially without change.

The problem at hand is to relate the noise fields at depth to the vertical atmospheric electric noise field, $E_{za}(0)$, which is assumed known at the earth's surface. Atmospheric noise typically propagates above the earth's surface as a TM mode with an incidence angle larger than, say, $70°$. Let the sine of this angle be denoted by S_a. The magnetic noise field at the surface is then given by

$$\mathcal{H}_{ya}(0) = E_{za}(0)/S_a \, .$$

(16)

The depth-dependent admittance seen by this signal can be computed by solving Eqs. (8) and (9), with $z_o = 0$, whence $S_o = S_a$ and $n_o = 1$. Note that no iteration is needed since S_a is specified, and only a single

integration of Eq. (9) is needed for each profile and wave frequency.
Once the admittance has been thus determined, the transfer functions,
Y_i, are easily computed from Eqs. (13) through (15). The resulting
equations are:

$$\mathcal{H}_{ya}(z) = Y_1 E_{za}(0), \tag{17a}$$

$$E_{za}(z) = Y_2 E_{za}(0), \tag{17b}$$

and

$$E_{xa}(z) = Y_3 E_{za}(0), \tag{17c}$$

where

$$Y_1 = \frac{1}{S_a} \exp\left[-ik \int_0^z dz' \ \frac{n^2(z')}{A(z')}\right], \tag{18a}$$

$$Y_2 = -\frac{S_a}{n^2(z)} Y_1, \tag{18b}$$

and

$$Y_3 = Y_1/A(z). \tag{18c}$$

Strictly speaking, the noise-transfer functions given above cannot be
completely specified, since the incidence angle (and, hence, S_a), is
never known precisely. However, these functions are very insensitive
to reasonable variations in S_a. For example, calculations for incidence
angles of 85° and 70° (a realistic range of values) yielded values for
Y_i that differed by less than 1 or 2 dB--an insignificant variation.
The results given in Sec. IV are computed for an assumed incidence angle
of 72° ($S_a = 0.95$), and should very accurately approximate the transfer
functions for all obliquely incident noise fields.

For propagation above the earth's surface and frequencies in the LF band and below, atmospheric noise is always much stronger than thermal noise; and above-ground long-wave systems are atmospherically noise limited. However, atmospheric noise is attenuated in the earth's crust and thus decreases with increasing depth; and thermal noise becomes greater with depth because of the higher temperatures. For certain situations, thermal noise could be the limiting factor for a deeply buried receiver. The thermal noise power density, N_T, will be computed from the simple relation

$$N_T = 1.38 \times 10^{-23} T \quad \text{watts/Hz} , \tag{19}$$

where T is the lithospheric temperature at the receiver depth in degrees Kelvin. T will be taken from the Keller model as shown in Fig. 2. Equation (19) for N_T is, of course, oversimplified. In a non-uniform medium such as the lithosphere, the antenna receiver "sees" a continuum of temperatures from the surrounding material. However, the error incurred by using Eq. (19) is quite small, as can be seen from the fact that the temperature varies by less than a factor of 2 (less than 3 dB) over the entire range of depths shown in Fig. 2. Further, other available lithospheric models show temperatures that differ from those shown in Fig. 2 by no more than 20 percent. *Gallawa and Haidle (1972)* have carried out detailed calculations of N_T, taking proper account of antenna directivity and integrating over the contribution from the surrounding medium. As would be expected from the above discussion, their results differ from those obtained from Eq. (19) by a few dB, at most. A few dB are insignificant compared with other factors that influence expected system performance.

ACHIEVABLE DATA RATES AND TRANSMISSION RANGE

The signal power at the receiver, S_{req}, required to achieve a data rate of R bits per second is given by

$$S_{req} = [E_b/N_{eff}]_{req} \, N_{eff} \, R \,, \tag{20}$$

where E_b is the energy per bit at the receiver, and N_{eff} is the effective (i.e., the post-processing) noise-power density. We assume $[E_b/N_{eff}]_{req} = 6$, which is sufficient to achieve an error rate of 10^{-3} with simple DPSK modulation. Equation (20) thus becomes

$$S_{req} = 6N_{eff} \, R \,. \tag{21}$$

For above-ground communications, it is customary to include a signal margin to insure reliability even during adverse fluctuations in propagation conditions. Such a margin has not been included in Eq. (21), because (unlike the ionosphere) the lithospheric waveguide should be a very stable communication channel.

In the following discussion, several idealizations are made to render the calculations of the received signal and noise tractable. These approximations are necessary because the problem of calculating the directivity and effective area of an antenna imbedded in a medium that is both conductive *and* inhomogeneous has never been solved. The directivity function of the receiving antenna is needed because the signal and atmospheric noise arrive from very different directions--the signal propagation being more or less lateral, whereas the atmospheric noise propagates mainly vertically in the earth's crust. We proceed with the calculation as if the receiving antenna were imbedded in a uniform medium. Although difficult to

justify rigorously, this approach should give a reasonably good estimate
of the required power. For all of the lithospheric models except one
(Levin "wet" model, Fig. 1), the refractive index in the crust is fairly
uniform and has a small imaginary part (implying a dielectric-like
medium) at depths where the conductivity is small and, hence, where a
receiver is apt to be placed. Moreover, although inaccurate in detail,
the expressions used do incorporate the important features of the
propagation and reception. For example, the expression used for antenna
directivity does correctly account for the fact that a vertical E-field
antenna is sensitive only to vertical electric fields, and thus mitigates
much of the atmospheric noise that is mainly horizontally polarized at
depth. The results thus should be adequate for this feasibility study.

For illustrative purposes, we assume that the receiving antenna is
a short, vertical electric dipole. This configuration is a logical
choice, since it should fit easily into a narrow, vertical borehole,
and will be relatively insensitive to downward propagating atmospheric
noise. Note that detailed antenna design is beyond the scope of this
study, and future study could well demonstrate that some other configura-
tion is more attractive. However, it is unlikely that alterations in
receiver design would change the forthcoming conclusions regarding system
feasibility. For example, any realistic antenna must be fairly small
electrically because of the large wavelengths in the crust (> 1-10km),
and all small antennas have about the same gain. Further, as is evident
from the numerical results given in Sec. IV, system feasibility is
dominated by the attenuation of the signal and atmospheric noise in the
crust. Neither of these factors depend in any way on hardware design.

For the effective area of the receiving antenna, we use

$$A_{eff}(z) \approx \frac{3/2 \pi \sin^2\theta}{\omega^2 \mu_0 \varepsilon_0 \varepsilon(z)} \quad (meters)^2 , \tag{22}$$

where the angle, θ, is measured relative to the vertical. The incident intensities I_s and I_a, associated with the signal and atmospheric noise density, respectively, are given by

$$I_s = 1/2 \sqrt{\varepsilon_0/\mu_0} \quad Re(n(z)) \ E^2(z) \quad watts/m^2 , \tag{23}$$

and

$$I_a = 1/2 \sqrt{\varepsilon_0/\mu_0} \quad Re(n(z)) \ E_a^2(z) \quad watts/m^2\text{-}Hz , \tag{24}$$

where E is the total signal electric field and E_a is the noise-field spectral density. Noting that $E^2 \sin^2\theta \simeq E_z^2$, etc., it follows that

$$\text{Signal Power} \simeq \frac{Re(n(z)) \ E_z^2(z)}{160 \ k^2 \varepsilon(z)} \quad watts , \tag{25}$$

and

$$\text{Atmospheric Noise Power Density} \simeq \frac{Re(n(z)) \ E_{za}^2(z)}{160 \ k^2 \varepsilon(z)} \quad watts/Hz ; \tag{26}$$

whereas the internal noise density is simply

$$N_T = 1.38 \times 10^{-23} \ TF \quad watts/Hz , \tag{27}$$

where F is the receiver-noise figure. The effective noise density at the receiver is thus

$$N_{eff} = \frac{Re(n(z))\ E_{za}^2(z)}{160\ k^2 \epsilon(z) G_p} + 1.38 \times 10^{-23} TF \quad watts/Hz\ , \qquad (28)$$

where G_p is the processing gain; i.e., the factor by which the effective atmospheric noise can be suppressed by using non-linear elements in the receiver circuit.

By inserting Eqs. (25) and (28) into Eq. (21), we find the following expression for the required vertical electric field at the receiver

$$(E^2(z))_{req} = \left| 6R\ \frac{E_{za}^2(z)}{G_p} + \frac{(160)(1.38 \times 10^{-23})k^2 \epsilon(z)}{Re(n(z))}\ TF \right|. \qquad (29)$$

The receiver is assumed to be at a depth, z. The final step for computing required power is to relate the signal electric field, $E_z(z)$, to the transmitter power. This can be done approximately by noting that the waveguide signal spreads nearly cylindrically from the source and also suffers an exponential attenuation given by Eq. (12). At a distance, d, from the receiver, the signal-power density can be written in the form

$$I_s \approx \frac{\eta P_o\ exp[-10^{-3}\alpha_N d/4.3]}{2\pi d\ h_{eff}}\ watts/m^2. \qquad (30)$$

Only a single waveguide mode (the Nth) has been used in Eq. (30), since we are considering distances large enough that only the least attenuated mode will contribute significantly. P_o is the total transmitter power, and η is the transmitter efficiency; *viz.*, the fraction of the total power that is radiated into the dominant (N^{th}) waveguide mode. The quantity h_{eff} is defined by

$$h_{eff} = \int_{-\infty}^{0} dz' \; \frac{Re(n(z)) \; E_z^2(z)}{Re(n(z_o)) \; E_z^2(z_o)} \tag{31}$$

and represents the nominal width of the waveguide region that contains most of the signal power. From Eqs. (17b), (23), and (29) through (31), it follows that for a receiver located at the "center" ($z=z_o$) of the waveguide, the required transmitter power is given by:

$$(P_o)_{req} \approx \frac{6\pi R h_{eff} d}{\eta} \left[\frac{Re(n_o) Y_2^2(z_o) \; E_{za}^2(0)}{120\pi \; G_p} + \left(\frac{4k^2 \epsilon(z_o)}{3\pi} \right) 1.38 \times 10^{-23} T(z_o) F \right]$$
$$\cdot \exp \left[\frac{10^{-3} \alpha_N d}{4.3} \right] . \tag{32}$$

For receiver depths other than z_o, the required power can be estimated from:

$$(P(z))_{req} = D(z) (P_o)_{req} , \tag{33}$$

where the depth degradation factor, D, is given by

$$D(z) = \frac{E_z^2(z_o)}{E_z^2(z)} \left\{ \frac{\dfrac{Re(n(z)) Y_2^2(z) E_{za}^2(0)}{120\pi \; G_p} + \left(\dfrac{4k^2 \epsilon(z)}{2\pi} \right) 1.38 \times 10^{-23} T(z) F}{\dfrac{Re(n(z_o)) Y_2^2(z_o) E_{za}^2(0)}{120\pi \; G_p} + \left(\dfrac{4k^2 \epsilon(z_o)}{3\pi} \right) 1.38 \times 10^{-23} T(z_o) F} \right\} \tag{34}$$

where z denotes the receiver depth, the transmitter depth being unspecified. For systems limited by atmospheric noise, D simplifies to

$$D(z) \approx \frac{E_z^2(z_o) \; \text{Re}(n(z)) \; Y_2^2(z)}{E_z^2(z) \; \text{Re}(n(z_o)) \; Y_2^2(z_o)} \; . \tag{35}$$

For systems limited by thermal noise:

$$D(z) \approx \frac{E_z^2(z_o) \; \epsilon(z) \; T(z)}{E_z^2(z) \; \epsilon(z_o) \; T(z_o)} \; . \tag{36}$$

The rationale used in selecting the various input parameters is discussed in Sec. IV.

IV. NUMERICAL RESULTS AND DISCUSSION

Pacific-Sierra's long-wave propagation code is used to calculate the attenuation rates, and the signal- and noise-wave functions, for several of the model waveguides shown in Figs. 1 through 3. The results of these calculations are given in this section. Detailed results are also given for the required power as a function of data rate, transmission range, and receiver burial depth. In all cases, the relative electric permittivity, ϵ, is assumed to have a constant value of ten.

ATTENUATION RATES

Figure 6 shows the calculated attenuation rates corresponding to the various model conductivity profiles. Results are shown only for the least-attenuated waveguide modes; viz., the TEM mode for frequencies lower than 3 or 4 kHz, and the lowest order TM mode for higher frequencies. The results showed that includion of only these modes is adequate for determining maximum transmission ranges. The decision to restrict attention to frequencies between 100 Hz and 100 kHz was somewhat, but not entirely, arbitrary. It is very difficult to radiate useful amounts of power at frequencies as low as 100 Hz. At frequencies higher than about 100 kHz, the computational methods used here become inconvenient due to the necessity of retaining large numbers of waveguide modes rather than the one or two least-attenuated ones. Ray-tracing methods are probably preferable to modal analysis at these higher frequencies. Also, the degrading effects of scattering from irregularities in the crust would be expected to become more pronounced. Nonetheless, it could well prove worthwhile to extend consideration to frequencies outside of the ELF/VLF/LF bands treated here.
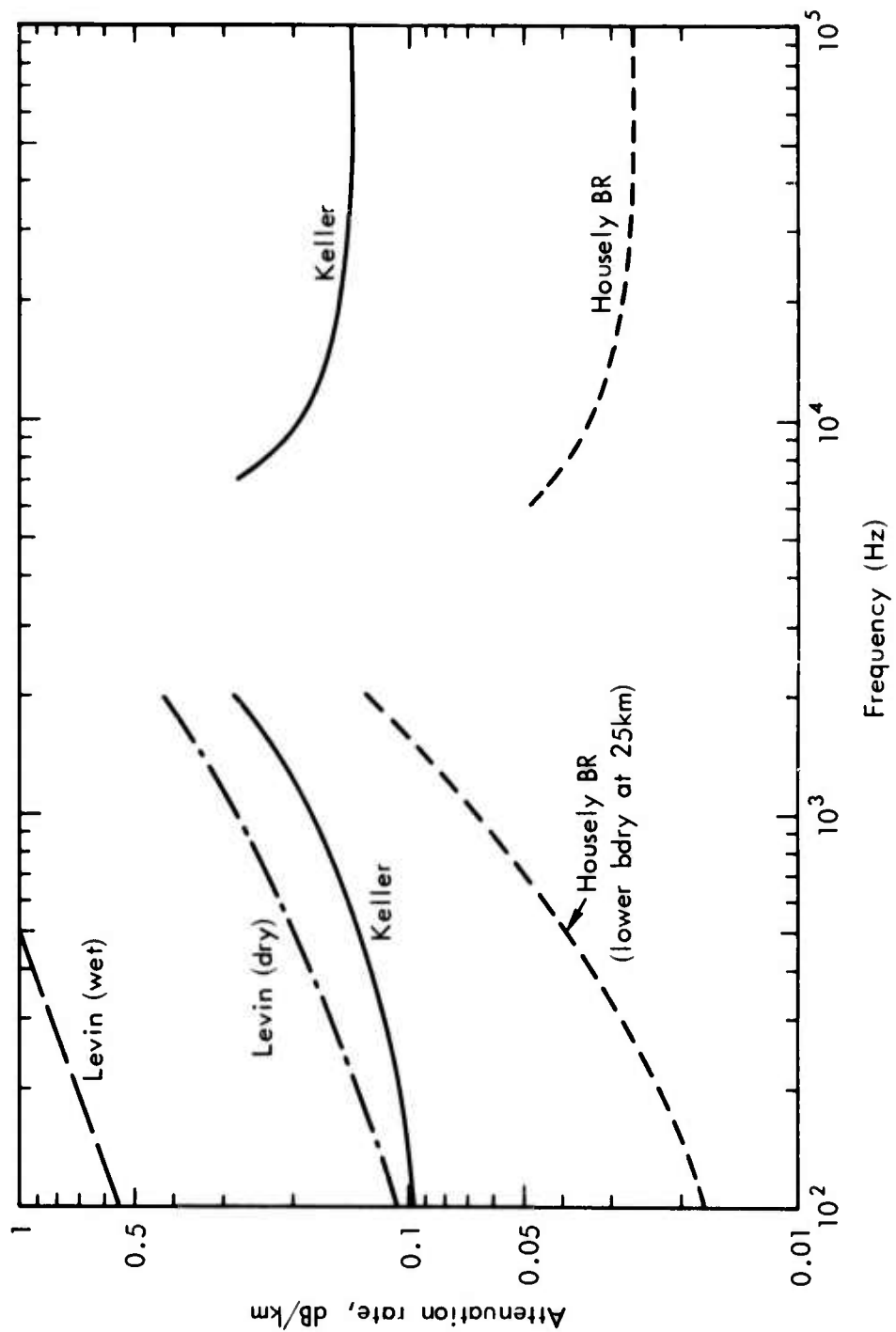
Fig. 6—Attenuation Rate vs. Frequency for Four Model Conductivity Profiles

The results shown in Fig. 6 apply to propagation in the continental lithosphere, since a transition to free space was assumed at z=0 (Fig. 5). Attenuation rates were also calculated for the case where the crust interfaces with sea water (approximated by a perfect conductor) at z=0. These results, which will not be presented in detail, are virtually identical to those shown in Fig. 6 for frequencies higher than a few hundred Hertz.[*] At lower frequencies, the effect of assuming a sea-water "top" on the waveguide is to reduce the attenuation from the values shown, particularly for the Keller and Housely BR models. This behavior is to be expected since, for extremely low frequencies where the skin depth is large, sea water reflects energy that would otherwise leak out of the waveguide.

The general dependence of attenuation on frequency, as shown in Fig. 6, is quite similar to that observed for long-wave propagation in the earth-ionosphere waveguide; viz., relatively low attenuation at frequencies less than a few hundred Hertz or higher than 10 kHz, and a "forbidden" band in the 1-to-5 kHz portion of the spectrum. However, in the earth-ionosphere waveguide, the attenuation rate is typically 2×10^{-3} to 4×10^{-3} dB/km in the VLF band. And the attenuation seldom exceeds 10^{-2} dB/km, even under disturbed ionospheric conditions. By comparison, the computed attenuations in the lithospheric waveguide are an order of magnitude or more larger.

The fact that the attenuation depends strongly on the minimum value of conductivity *and* the conductivity depth-gradients is clearly illustrated by the results shown in Fig. 6. The minimum conductivity is

---

[*] The reader is cautioned against applying these results to propagation under the oceans, however, since the models shown in Figs. 1 through 3 were developed to represent the continental lithosphere.

about 10^{-5} mhos/m for the Levin (wet) model, about 10^{-7} mhos/m for both the Levin (dry) and Keller models, and about 5×10^{-9} mhos/m for the Housley BR model. As would be expected, the Housley BR model yielded the lowest attenuation, whereas that yielded by the Levin (wet) model was by far the highest. However, the attenuation rates for the Levin (dry) model and the Keller model are quite different, even though the minimum conductivity is nearly the same for the two models. At a frequency of 1 kHz, the calculated attenuation rate is about 0.18 dB/km for the Keller model and about 0.28 dB/km for the Levin (dry) model. The more favorable attenuation in the Keller model of the lithospheric waveguide is due in part to the assumed presence of a rapid transition in conductivity at a depth of about 14 km (Fig. 2).

It is interesting to compare the results shown in Fig. 6 with the attenuation rates computed by *Spies and Wait (1971)* for a step-function model of the conductivity depth-profile. For an assumed waveguide conductivity of 10^{-7} mhos/m, their calculated attenuation rates are typically a factor of two or three lower than those shown in Fig. 6 for the Keller and/or Levin (dry) models. These lower attenuation rates are due largely to Spies and Wait's use of sharp, highly reflecting upper and lower boundaries rather than the gradual "boundaries" used here. Of course, the conductivities used by Spies and Wait in their step-function representation of the waveguide are intended to be "effective" values, averaged over some appropriate range of depths, rather than minimum values. In this context, the effective conductivity of the Keller-model waveguide would be, say, 5 or 6×10^{-7} mhos/m, even though the minimum conductivity is about 10^{-7} mhos/m.

The significant effect of conductivity depth-gradients, and the presence or absence of sharp transitions in the conductivity depth-profile, can be illustrated by examining the Housley BR model more closely. For reasons discussed in Secs. II and III, the results shown in Fig. 6 are not computed for the Housley BR model precisely as shown in Fig. 3 (p. 13). Instead, the conductivity values shown are used for depths down to 25 km, where a sharp transition to a highly conducting sub-basement (i.e., a highly reflecting "boundary") is assumed. As a check on sensitivity, additional calculations of the attenuation rates for the Housley BR model are carried out for assumed lower "boundary" depths other than 25 km. Sample results are given in Fig. 7 for a frequency of 1 kHz. The attenuation is seen to increase markedly as the assumed layer depth is increased. Results corresponding to the Housley BR profile, precisely as shown in Fig. 3, can be obtained by taking the depth of the assumed "boundary" to be infinite. For this case (see Fig. 7), the attenuation rate is about twice as large as when the profile is terminated at 25 km,[*] and is nearly as large as for the Keller model (see Fig. 6). Of course, if the assumed transition at 14-km depth were removed from the Keller model, or if it were assumed to occur at a greater depth, then the calculated attenuation rates would be larger than shown in Fig. 6.

---

[*] It should not be inferred from Fig. 7 that the placement of the reflecting layer at a depth of 25 km causes the results shown in Fig. 6 (and to be shown below in figures for the Housley BR model) to be unduly optimistic. It can be inferred from seismic data that, for many regions, a highly reflecting transition exists at depths shallower than 25 km, in which case the Housley BR results would be more favorable than those on which the conclusions of this report are based.
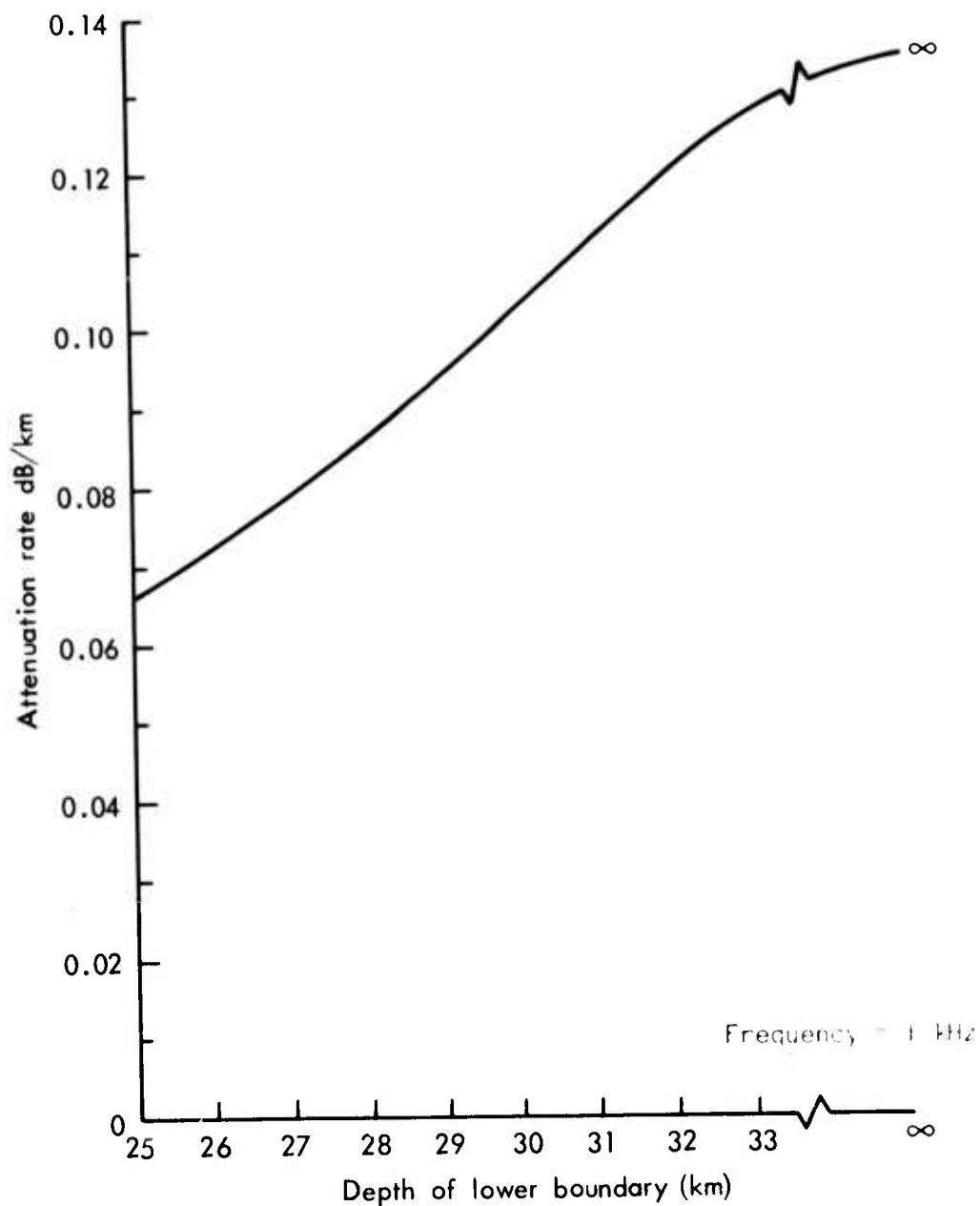
Fig. 7--Attenuation Rate vs. Depth of Assumed Sharp
Transition in Conductivity (Housley BR Profile)

SIGNAL AND NOISE FIELD-STRENGTH PROFILES

Equations (13) through (15) have been integrated to obtain the field-strength profiles associated with the least attenuated waveguide modes. Figures 8 and 9 show sample results, illustrating the calculated field-strength profiles for the Keller model and frequencies of 1 kHz (TEM mode) and 10 kHz (TM mode). Recall that in all cases the fields are normalized such that $\mathcal{N} = 1$ at the "center" of the waveguide; i.e., at the depth of minimum conductivity. Thus, for the Keller model, $\mathcal{N}$ has been set equal to unity at a depth of about 10 km.

One of the goals of this study is to estimate the dependence of expected system performance on the burial depth of the receiving antenna. Thus, for a vertically oriented E-field receiver--the configuration assumed for illustrative purposes--the depth dependence of $|E_z|$ is of particular interest. Figures 8 and 9 show that $|E_z|$ has a broad maximum centered at a depth of about 10 km. However, for depths shallower than 5 or 6 km, $|E_z|$ decreases rapidly as the depth is decreased. This behavior, which is characteristic of a trapped mode in a waveguide "centered" at a depth of 10 km, is due to four physical effects: 1) energy is absorbed as the signal propagates upwards toward the earth's surface; 2) the conductivity and, hence, the admittance of the medium increases as the depth is reduced--causing the electric fields to be reduced relative to the magnetic field; 3) the signal suffers gradient reflection as it "tries" to propagate upwards; 4) since the refractive index increases as the depth is reduced, the
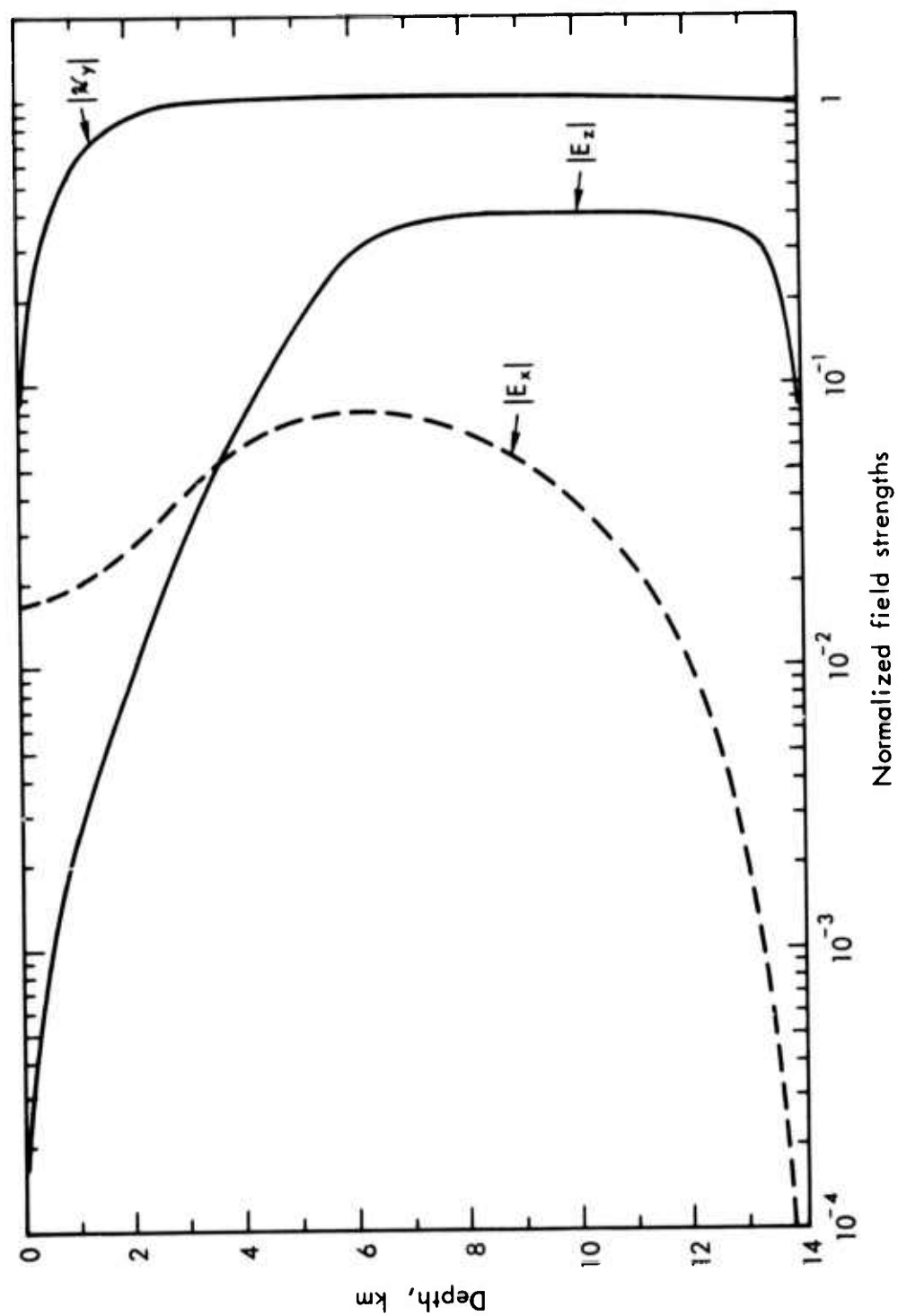
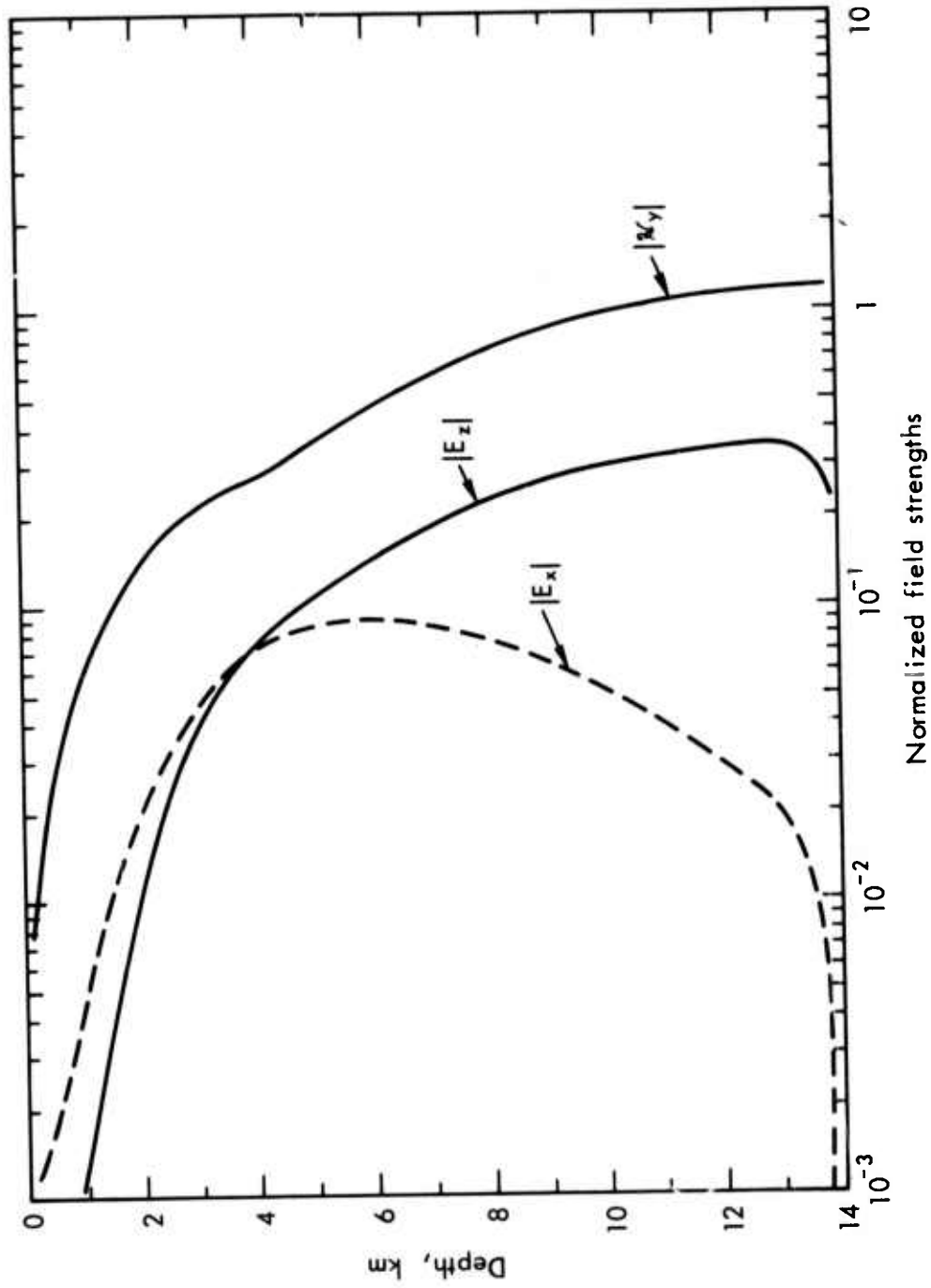Fig. 8—Normalized Field Strengths vs. Depth (Keller Profile, 1 kHz)

Fig. 9--Normalized Field Strengths vs. Depth (Keiler Model, 10 kHz)

"wave" normal becomes more nearly vertical as the signal propagates

upward.[*] This effect causes $|E_z|$ to be reduced relative to both $|E_x|$

and $|\mathscr{N}_y|$. For depths greater than about 4 km and the two frequencies

corresponding to Figs. 8 and 9, $|E_z|$ is greater than $|E_x|$, which

indicates a signal traveling mainly in a horizontal direction. At

depths shallower than 4 km, the propagation direction has become more

nearly vertical than horizontal. Of the four effects described above,

absorption becomes relatively more important as the frequency is

increased, since the skin depths are reduced, as are the admittances

and refractive indices.

Figure 10 shows the frequency dependence of the relative vertical

electric field strength a several depths for the Keller model. As

indicated on the figure, the relative field strength is normalized to

unity at a dep. of 10 km. As would be expected, the relative field

strength becomes smaller as the depth becomes shallower. Field-strength

profiles have also been calculated for the Housely and Levin models,

but in the interest of brevity are not presented in detail. For depths

shallower than about 10 km, the field-strength profiles based on the

Housley BR model are very nearly the same as those shown for the Keller

profile. This similarity is to be expected, of course, since the

conductivity profiles in the two models are identical for most of the

0-to-10 km depth range. On the other hand, the Levin (dry) model is

---

[*] This interpretation is intended solely to provide an intuitive
understanding of the numerical results and should not be taken too
literally. Strictly speaking, of course, the concepts of wave normal
and propagation direction do not apply when the medium has large spatial
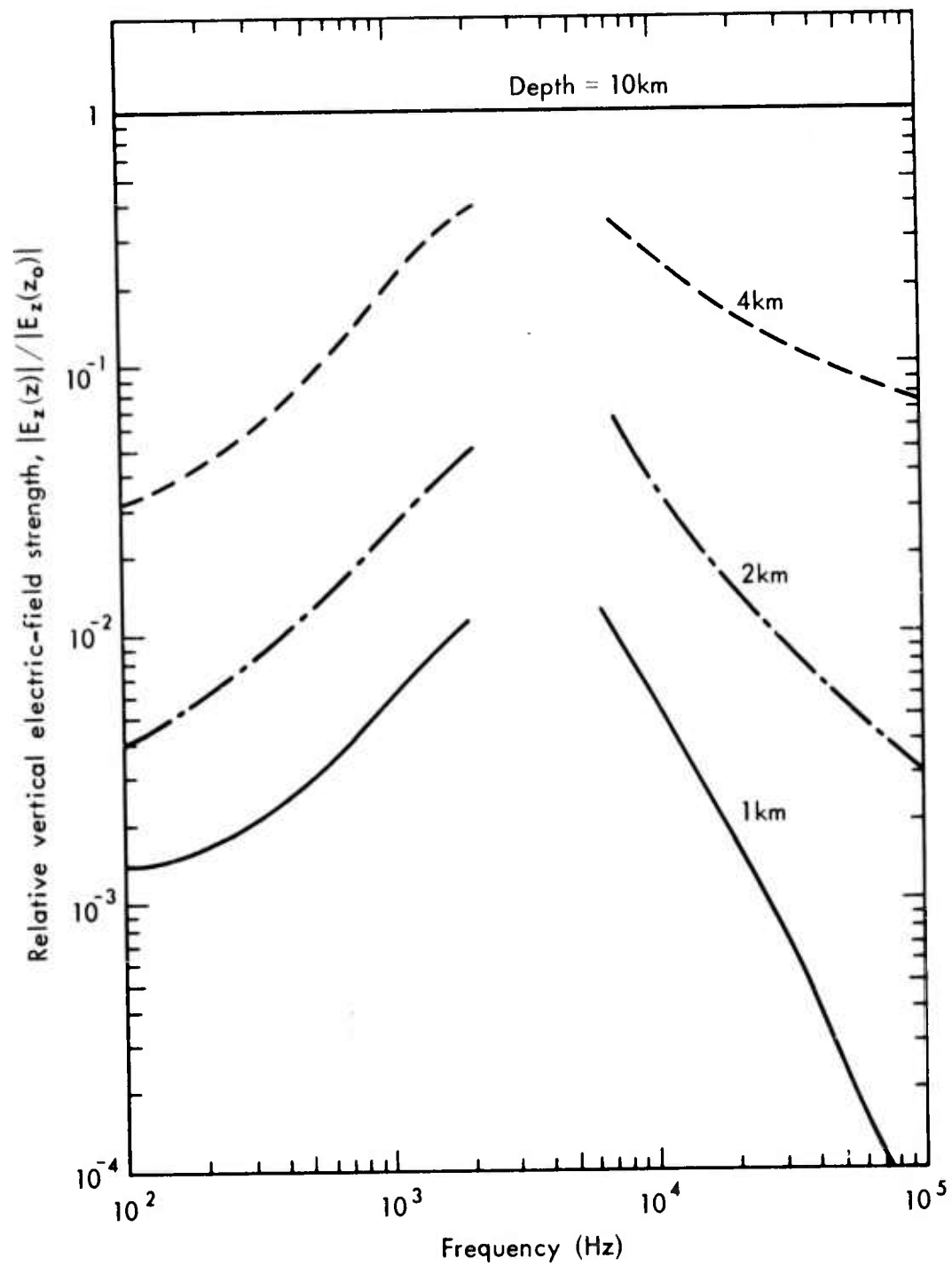gradients, as is the case here.

Fig. 10--Relative Vertical Electric-Field Strength vs.
Frequency for Several Depths (Keller Profile)

seen (Fig. 1, p. 9) to be much more highly conductive than either the Keller or the Housley models for depths shallower than about 8 km. Consequently, for depths shallower than 8 km, the relative field strengths for the Levin (dry) profile are orders of magnitude smaller than those shown in Figs. 8 through 10.

Noise-transfer functions have been computed from Eq. (18). Figures 11 and 12 show $|Y_2|$ and $|Y_3|$ as a function of depth for the Keller model, and frequencies of 1 kHz and 10 kHz. Recall that the surface-noise fields shown in Fig. 4 should be multiplied by $|Y_2|$ or $|Y_3|$ to obtain the vertical or horizontal electric-noise fields, respectively, at a given depth. The noise propagates downward from the earth's surface, whereas the signal propagates upward (and laterally) from the center of the waveguide. Thus, absorption and reflection tend to *reduce* $|Y_2|$ and $|Y_3|$ as the depth is increased. This behavior is different than noted above for the signal fields, which suffer reflection and reflection losses as the depth is decreased. These statements do not imply that the transfer functions must necessarily decrease monotonically with increasing depth. As illustrated by Fig. 11, for example, refractive effects can be dominant at the lower frequencies and actually cause $|Y_2|$ to have a larger value near the center of the waveguide than near the earth's surface. Further, since the conductivity becomes low near the center of the waveguide, the crust becomes quite transparent at these depths and standing wave patterns in the transfer functions can occur. An example of such a pattern is shown in Fig. 13.
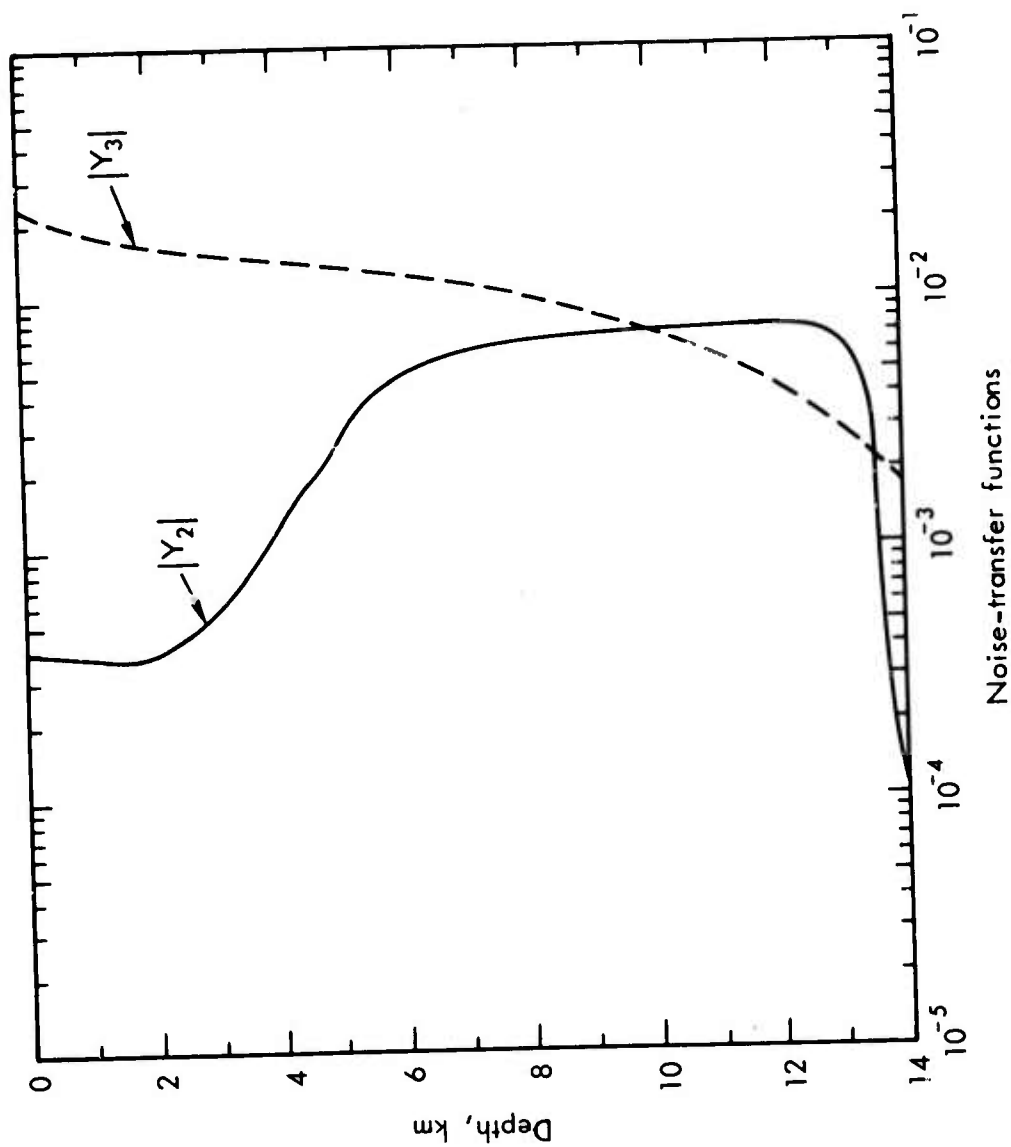
Fig. 11--Noise-Transfer Functions vs. Depth (Keller Profile, 1 kHz)
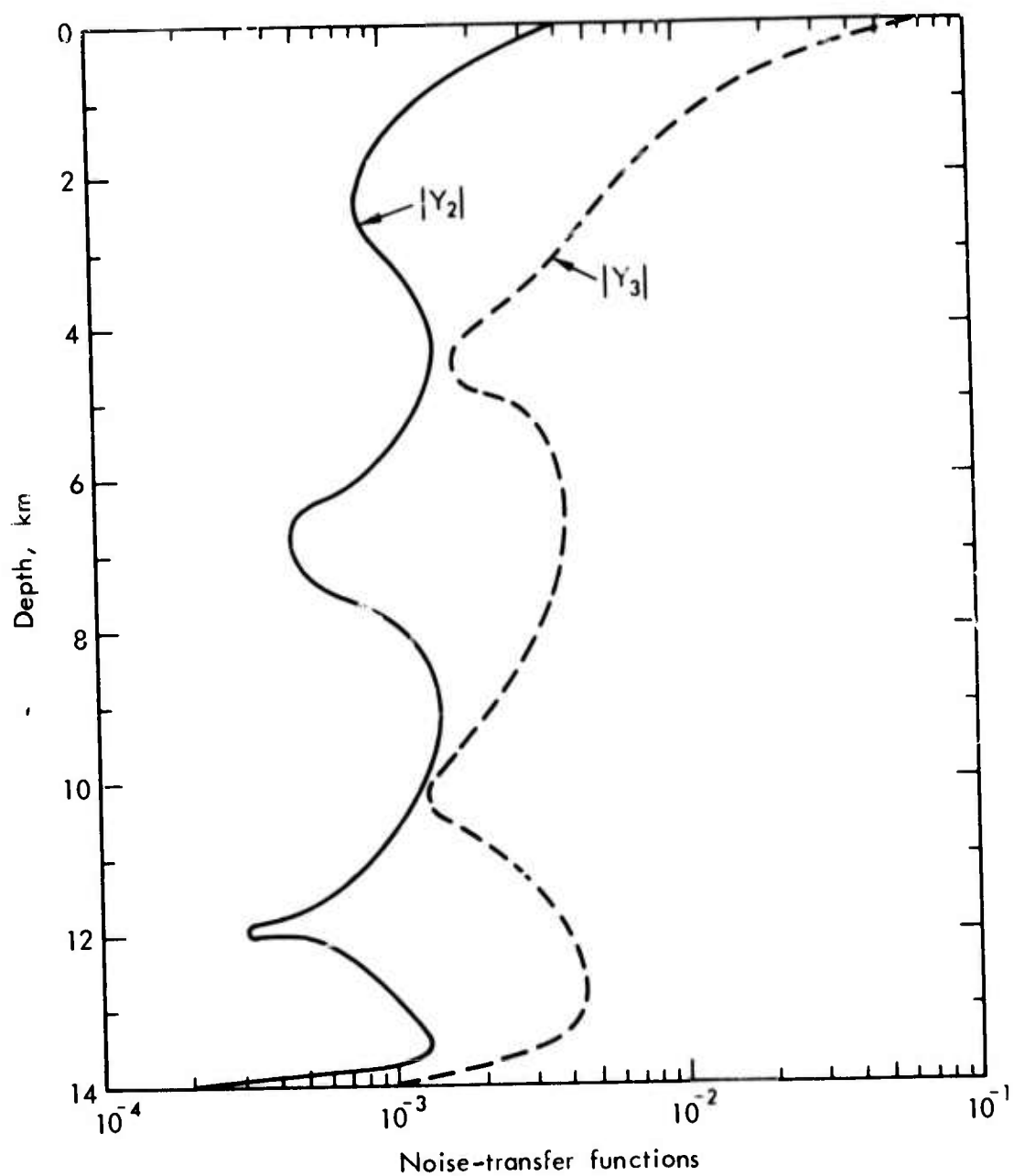
Fig. 12--Noise-Transfer Function vs. Depth (Keller Profile, 10 kHz)

Figures 11 and 12 show that $|Y_2|$ is considerably smaller than $|Y_3|$ for most depths of interest. This behavior was found to occur for essentially all of the models and frequencies for which calculations were made. Thus, at least for the models used here, the vertical noise electric-field component is typically much smaller than the horizontal one; and a vertically oriented electric antenna should therefore be less severely degraded by atmospheric noise at depth than a horizontally oriented one. This distinction has often been overlooked (e.g., *Gallawa and Haidle, 1972*), and occurs simply because low-frequency electromagnetic waves tend to be refracted strongly toward the vertical upon entering the earth from free space.

The frequency dependence of the noise-transfer function of interest, $|Y_2|$, is shown in Fig. 13 for the Keller model at several depths. At the lowest frequencies considered, the vertical component of atmospheric noise tends to increase with increasing depth, indicating a dominance of refraction over absorption. Thus, somewhat surprisingly, the vertical component of atmospheric noise at ELF is found to be stronger at a depth of 10 km than at a depth of, say, 2 km. Of course the *total* normalized noise power decreases more-or-less monotonically with increasing depth. At the higher frequencies, $|Y_2|$ is seen to decrease as the depth is increased, indicating that absorption is the dominant mechanism determining field strength.

DEPENDENCE OF SIGNAL-TO-NOISE RATIO ON RECEIVER DEPTH

We next consider the depth-degradation factor, $D(z)$, which is simply the ratio of the signal-to-noise ratio at a given depth to that
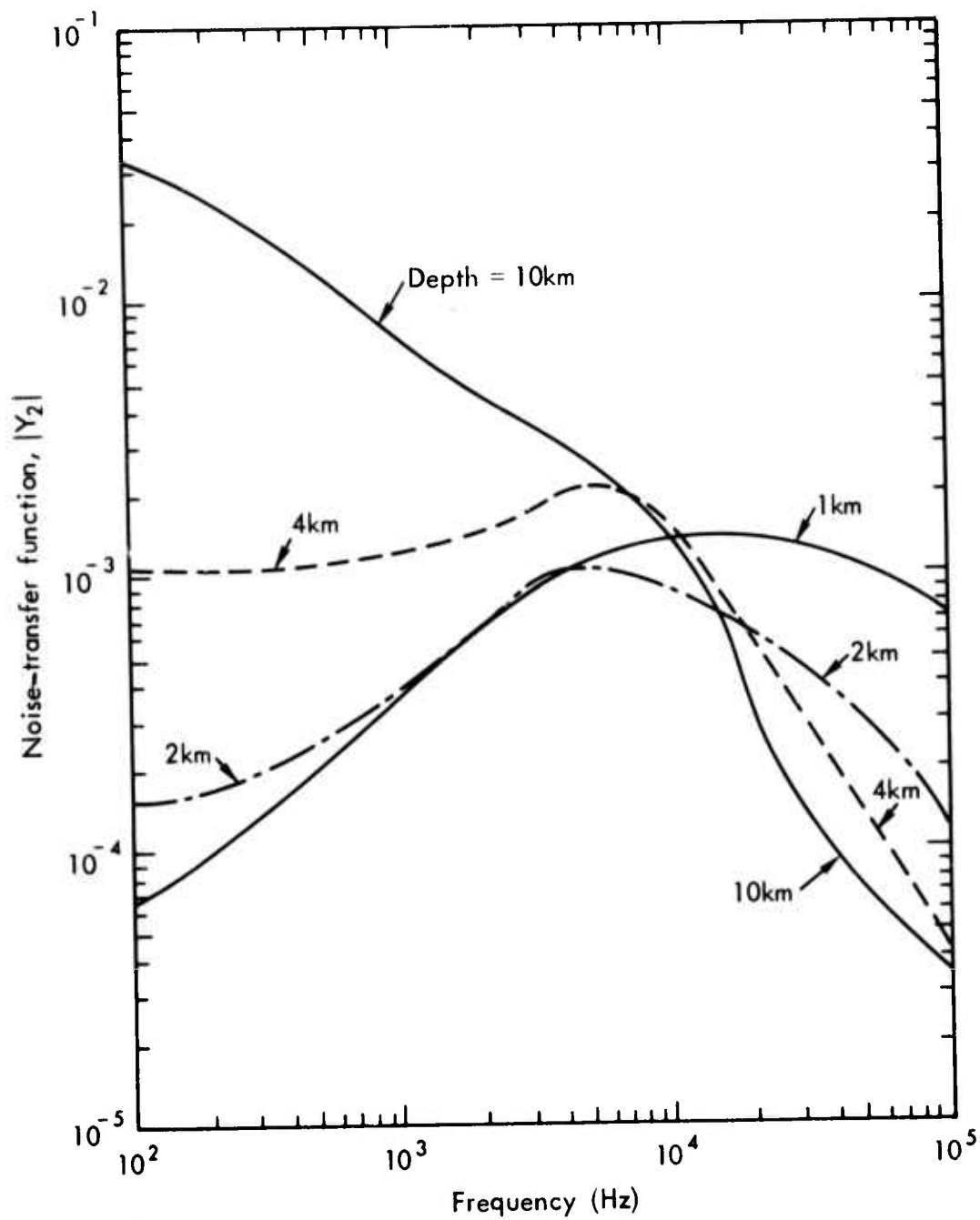
Fig. 13--Noise-Transfer Function (Vertical E-field) vs. Frequency
for Several Depths (Keller Profile)

at the nominal center of the waveguide. Thus, in the Keller model, for example, $D(z)$ is the power required to transmit to a receiver at a depth, z, divided by the power required to transmit to a similar receiver buried at a depth of 10 km; i.e., $D(z)$ is the factor by which the transmitter power must be changed if the receiver is moved from a 10-km depth (Keller model) to some other depth. Since 10-km deep holes are very expensive to bore, we are particularly interested in determining the additional power that would be required if the receiver were placed at some lesser depth.

For all of the models considered in this report, atmospheric noise dominates the thermal noise for all depths and frequencies of interest.[*] Thus, the simplified Eq. (35) may be used, and $D(z)$ expressed solely as a function of the signal field-strength profiles and $|Y_2|$. Some examples of the depth-degradation factor are given for the Keller model (1 and 10 kHz) and the Levin (dry) model (1 kHz) in Fig. 14. For the Keller model, which exhibits a fairly constant conductivity depth-gradient between 0 and 10 km, relatively little degradation would be suffered by reducing the receiver depth from 10 km to, say, 5 or 6 km. Moreover, as discussed below, the penalty in transmission range is remarkably moderate even for receiver depths as shallow as 3 km. As indicated earlier, the Levin (dry) model exhibits a rather large and abrupt

---

[*] This dominance occurs because, even after allowing for losses suffered in propagating from the earth's surface to the nominal center of the waveguide, the atmospheric-noise density was found to be stronger than the thermal-noise density. It is, of course, possible to envision realistic situations in which the atmospheric noise would be so highly attenuated as to be no longer dominant. A case in point would be if the receiver were situated in the suboceanic lithosphere.
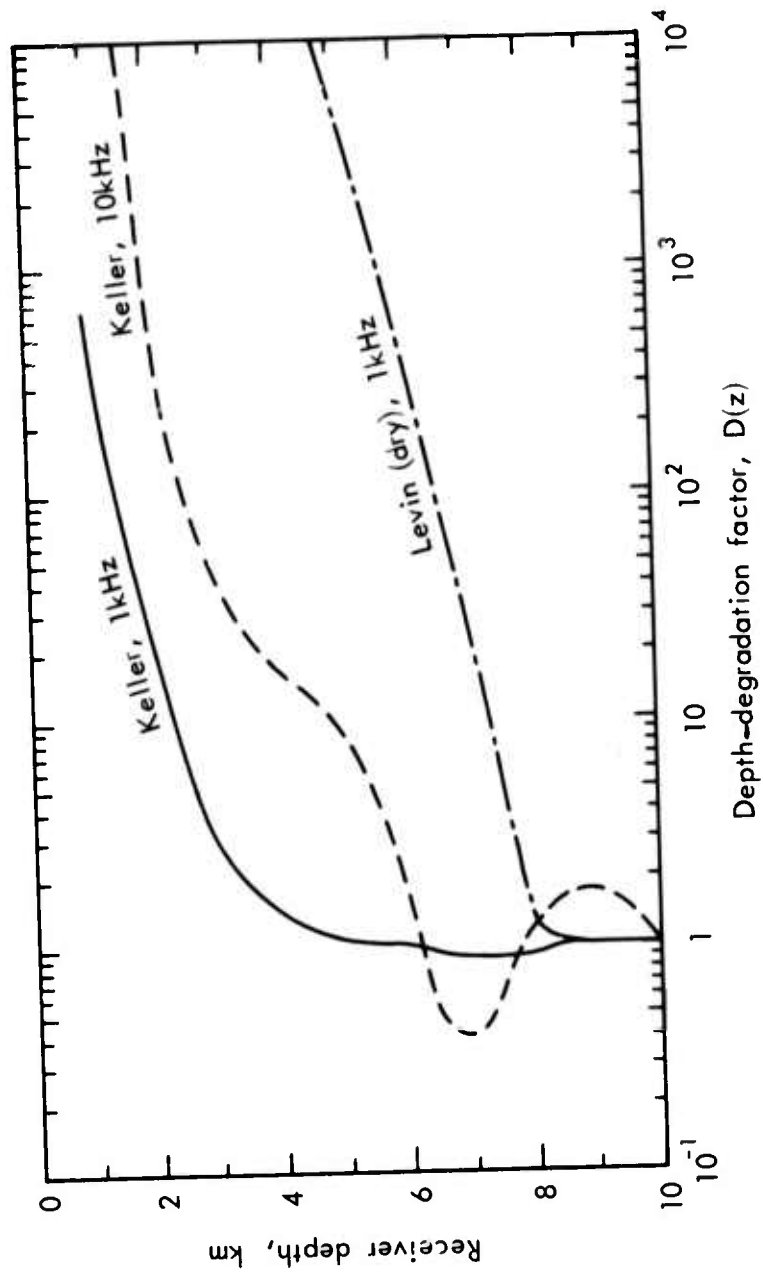
Fig. 14--Depth-Degradation Factor vs. Receiver Depth

increase in conductivity as the depth is reduced to less than about 8 km.[*] A major result of this assumed transition in conductivity is illustrated in Fig. 14; $D(z)$ becomes so large as to essentially rule out any possibility of using a receiver depth shallower than 7 or 8 km. Thus, to the extent that borehole depth affects total system cost, the attractiveness of a lithospheric communication system depends quite strongly on the gradient of conductivity in the crust at depths between 0 and 10 km.

Figure 15 shows the frequency dependence of $D(z)$ for the Keller model and several depths of interest. Of course, $D(z)=1$ at a depth of 10 km. As might be expected, higher frequency signals are much more sensitive to receiver burial depth than are lower frequency ones. The large increase in $D(z)$ for shallow depths exhibited at frequencies higher than 10 kHz is due to two factors: 1) the signal gets weaker as the surface of the earth is approached, due to absorption suffered in propagating upward from near the center of the waveguide; 2) the atmospheric noise gets stronger near the earth's surface, since the absorption it suffers in propagating downward is reduced. For reasons given above, $D(z)$ for the Housley BR model is very nearly the same as that shown in Fig. 15, whereas that for the Levin model is prohibitively large at depths shallower than 7 or 8 km.

TRANSMISSION RANGES AND POWER REQUIREMENTS

The dependence of required power on data rate, transmission range, transmitter efficiency, frequency, and receiver burial depth has been

---

[*] This behavior would be expected in regions having a thick, highly conducting, sedimentary layer.
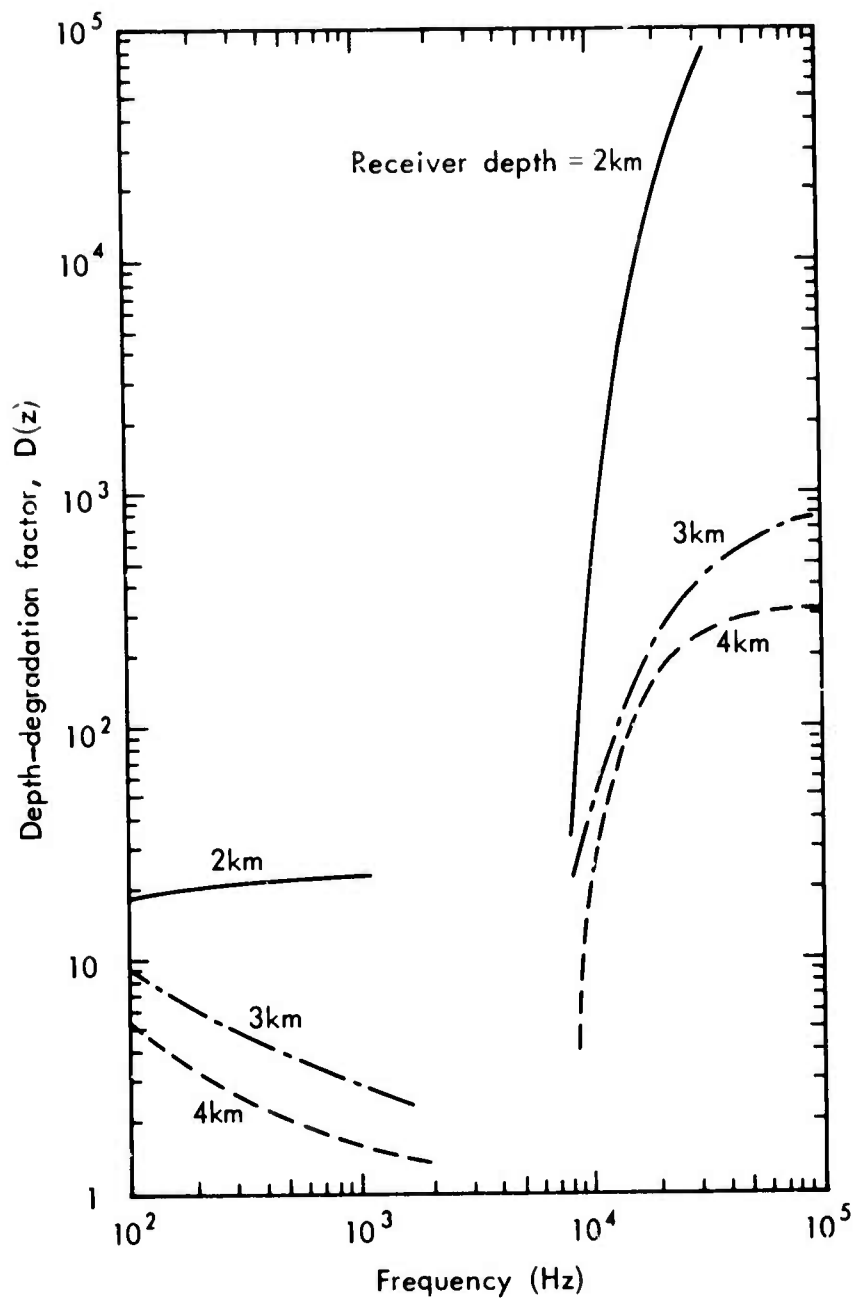
Fig. 15--Depth Degradation vs. Frequency for Several Receiver Depths (Keller Profile)

calculated from Eqs. 32 and 33. Values for rms atmospheric noise corresponding to Colorado summer are taken from Fig. 4, (p. 15). As discussed in Sec. II, the use of rms noise spectra implies a system time availability of 80-to-90 percent. Also, we assume no processing gain, and have thus taken G_p equal to unity. This assumption is probably quite conservative, since 10-to-20 dB of noise suppression can typically be achieved in above-ground VLF/ELF systems (*Evans and Griffiths, 1972*). If, say, 10 dB of noise suppression can be achieved in a lithospheric system, then the power requirements given below would suffice for a time availability approaching 99 percent, rather than the above-stated 80-to-90 percent. For purposes of presentation, it is convenient to define a normalized, required effective power (REP) as follows:

$$REP = \frac{\eta \, P_{req}}{R} \quad \text{(Watts)}, \tag{37}$$

where P_{req} is the total power that must be delivered by the transmitter,[*] as computed from Eq. (33). The transmitter efficiency, η, denotes total efficiency; viz., the ratio of the power radiated into the least-attenuated mode to the total system power; η thus accounts for antenna radiation efficiency, the excitation efficiency of the dominant waveguide mode, transmission line losses, etc. Therefore, REP denotes

---

[*] Strictly speaking, REP has units of Joules/bit, rather than Watts, since R has units of bits-per-sec, and η is dimensionless. The distinction vanishes for a data rate of 1 bps, since the energy per bit is then numerically equal to the power. A more precise definition than given by Eq. 37 would be

$$REP = \frac{\eta \, R_o}{R} \, P_{req} \, ,$$

where $R_o = 1$ bit-per-second. In the following discussion and figures, the factor R_o is suppressed, and REP will be expressed as the effective power required to transmit 1 bit-per-second.

the power that must be radiated into the dominant mode to achieve a data rate of 1 bit-per-second (bps). REP is a convenient parameter, since it is independent of η (see Eq. 32), which is extremely difficult to calculate for a transmitter in an inhomogeneous conducting medium. It is, of course, a simple matter to compute the required power, P_{req}, from REP, once η has been calculated and a data rate, R, chosen.

The transmitter efficiency, η, cannot now be specified accurately. However, some assumption must be made regarding achievable transmitter efficiencies if system feasibility and attractiveness are to be assessed quantitatively. To undertake such an assessment, we assume, without delving into the specific transmitter configuration, an efficiency that, based upon present understanding, does not appear to be unduly optimistic. Specifically, in addition to detailed calculations of REP, results will be given for P_{req} for the case where $\eta/R = 10^{-3}$; i.e., where the total required power exceeds REP by a factor of 1000. This choice is by no means arbitrary. *Gallawa and Haidle (1972)* have estimated that efficiencies of a few percent should be achievable for a VLF transmitter utilizing a deeply buried vertical antenna. Thus, at VLF, our choice of $\eta/R = 10^{-3}$ can be interpreted as corresponding to an efficiency of a few percent and a data rate of a few tens of bps. Of course, for poorer efficiencies, such as would probably occur at the lower frequencies considered, the data rates would be proportionately lower. Although we consider $\eta/R = 10^{-3}$ to be a reasonable choice for the purposes of this study, other values could equally well have been used. Fortunately, the main conclusions do not depend strongly on the precise value of η. Moreover, since extensive graphs of REP are

given below, total power requirements can be obtained for any efficiency and data rate: simply multiply REP by R and divide by η.

Figure 16 shows REP as a function of transmission range for several frequencies and the Keller model. For comparison, REP for the Levin (dry) model is shown for a frequency of 1 Hz. The results shown in Fig. 16 apply to the situation where the receiving antenna is located near the center of the waveguide--about 10-km deep for the Keller model and about 9-km deep for the Levin (dry) model. Also shown in Fig. 16 (right-hand axis) is the total required system power for combinations of efficiency, η,[*] and data rate, R, such that $\eta/R=10^{-3}$. Any effects of transmitter burial depths are included implicitly in the efficiency, η.

Several important conclusions can be drawn from Fig. 16. The higher frequencies considered are clearly superior to the lower ones, as evidenced by the fact that, for a given power, far greater ranges are achievable at 50 kHz than at the other frequencies shown. This superiority is almost entirely due to the quieter noise environment at 50 kHz and a depth of 10 km. Reference to Fig. 13 shows that, for a depth of 10 km, the noise-transfer function, $|Y_2|$, decreases strongly and monotonically with increasing frequency. Actually, the superiority of the higher frequencies is probably even more clear-cut than shown in Fig. 16--it should be easier to achieve $\eta/R=10^{-3}$ at 50 kHz than, say, at 1 kHz, since antenna efficiencies typically increase with increasing frequency.

---

[*] We do not imply, of course, that η will be independent of frequency and receiver burial depth.
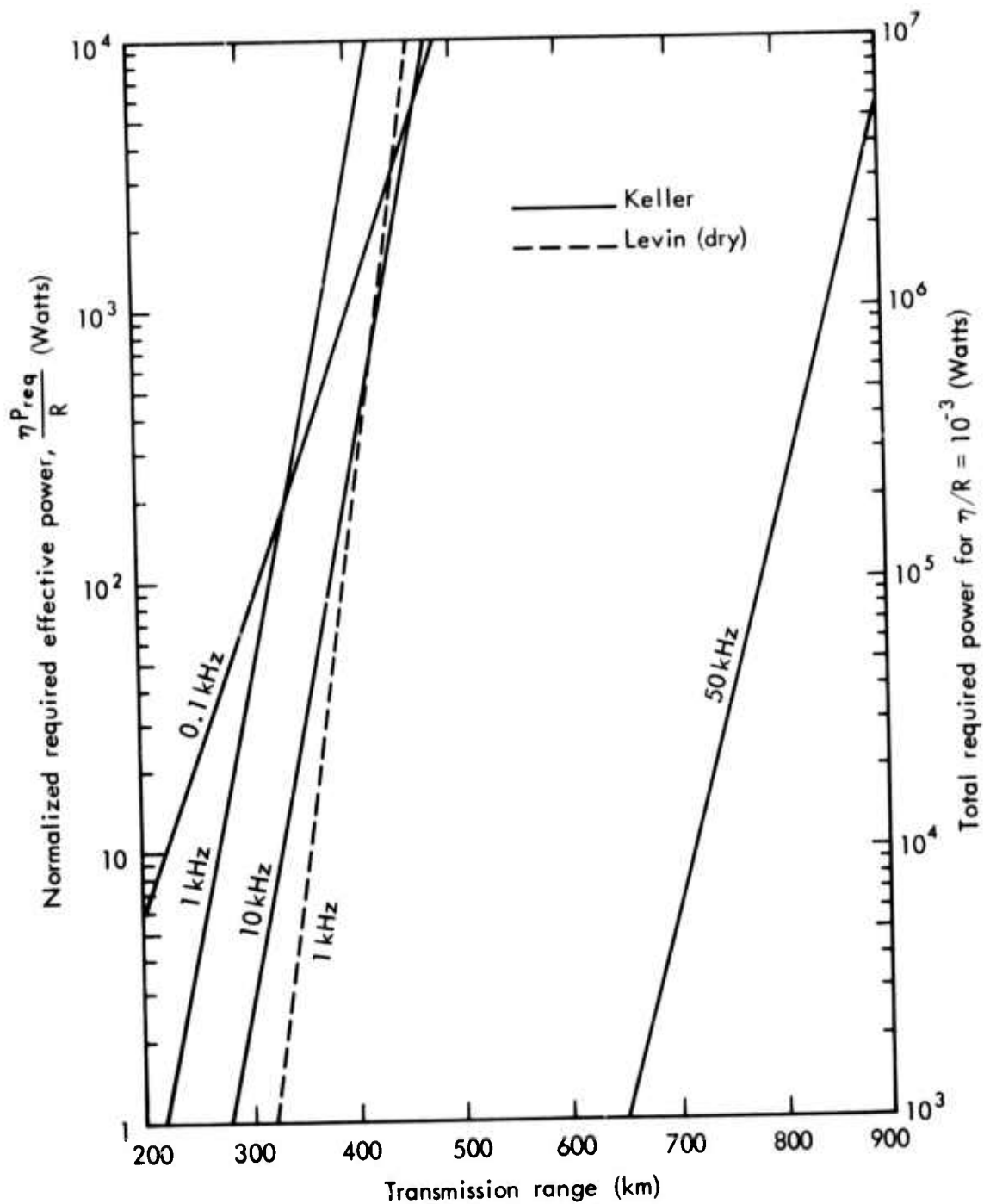
Fig. 16--Transmission Range vs. Effective Power and Total Power
(Keller and Levin (dry) Profiles, 10-km Receiver Depth)

For purposes of discussion, we assume that 10 megawatts is an acceptable power requirement for a practical system. On this basis, transmission ranges on the order of 1000 km appear achievable, provided that the Keller (or Levin (dry)) model of the lithosphere is found through field measurements to be a reasonably good representation. On the other hand, the system power requirement based on the Levin (wet) model are so high for transmission ranges of interest that the results are not even worth presenting.

One very important general point should be noted: viz., the system performance depends exponentially on signal- and noise-attenuation rates, but only linearly on other parameters. Thus, the required power at a given frequency depends linearly on η and R, and exponentially on the transmission range, d. Conversely, achievable transmission range depends only logarithmically on efficiency, data rate, and power. A misleading impression can be gained if system performance is assessed on the basis of the power required to transmit to some specified range. Instead, performance should be assessed on the basis of the range that can be attained with some specified power. The following simple numerical example will clarify the distinction: As indicated above for the Keller model, a range of 1000 km is attainable with a total power of 10 megawatts, provided that $\eta/R=10^{-3}$. Assume, for purposes of discussion, that future analysis shows that $\eta/R=10^{-4}$ is the best that can be achieved. If the 1000-km transmission range is regarded as specified, then the power requirement increases to 100 megawatts, which is probably impractical. On the other hand, if the 10-megawatt power is regarded as specified,

then the ten-fold decrease in efficiency[*] causes the maximum transmission range to decrease to about 850 km--a penalty of only 15 percent.

Since system cost will depend greatly on the depth to which antennas must be buried, we next consider the penalty in *transmission range* (power being specified) that must be paid if receiving antennas are buried shallower than the nominal center of the waveguide. Since practical radio communication systems typically have many more receivers than transmitters, receiver burial depth is probably a more important consideration than transmitter burial depth.

Figure 17 shows, for the Keller model and frequencies of 10 and 50 kHz, the dependence of required power on transmission range for several assumed receiver burial depths. For a frequency of 50 kHz and a total power of 10 megawatts, the calculated transmission ranges are 700-to-800 km for receiver depths as shallow as 3 or 4 km. These ranges are only 20-to-30 percent less than those corresponding to a receiver depth of 10 km.[**] Since drilling costs are apt to be a large fraction of the total system cost, a tradeoff of a 20-to-30 percent reduction in transmission range against a factor of 3 reduction in borehole depth would seem advisable. Such a tradeoff cannot be carried too far, however. For the Keller model and a frequency of 50 kHz, use of a receiver depth of only 2 km would cause the depth degradation function (Figs. 14 and 15) to

---

[*]Or, equivalently, a ten-fold increase in required data rate, or ten-fold decrease in allowable system power.

[**]Again note the misleading conclusions that can be drawn if transmission range, rather than power, is considered to be a system specification. For a *given* range and a frequency of 50 kHz, reduction of the receiver depth from 10 km to 3 km would necessitate an increase in power of nearly 3 orders of magnitude (for the Keller model)!
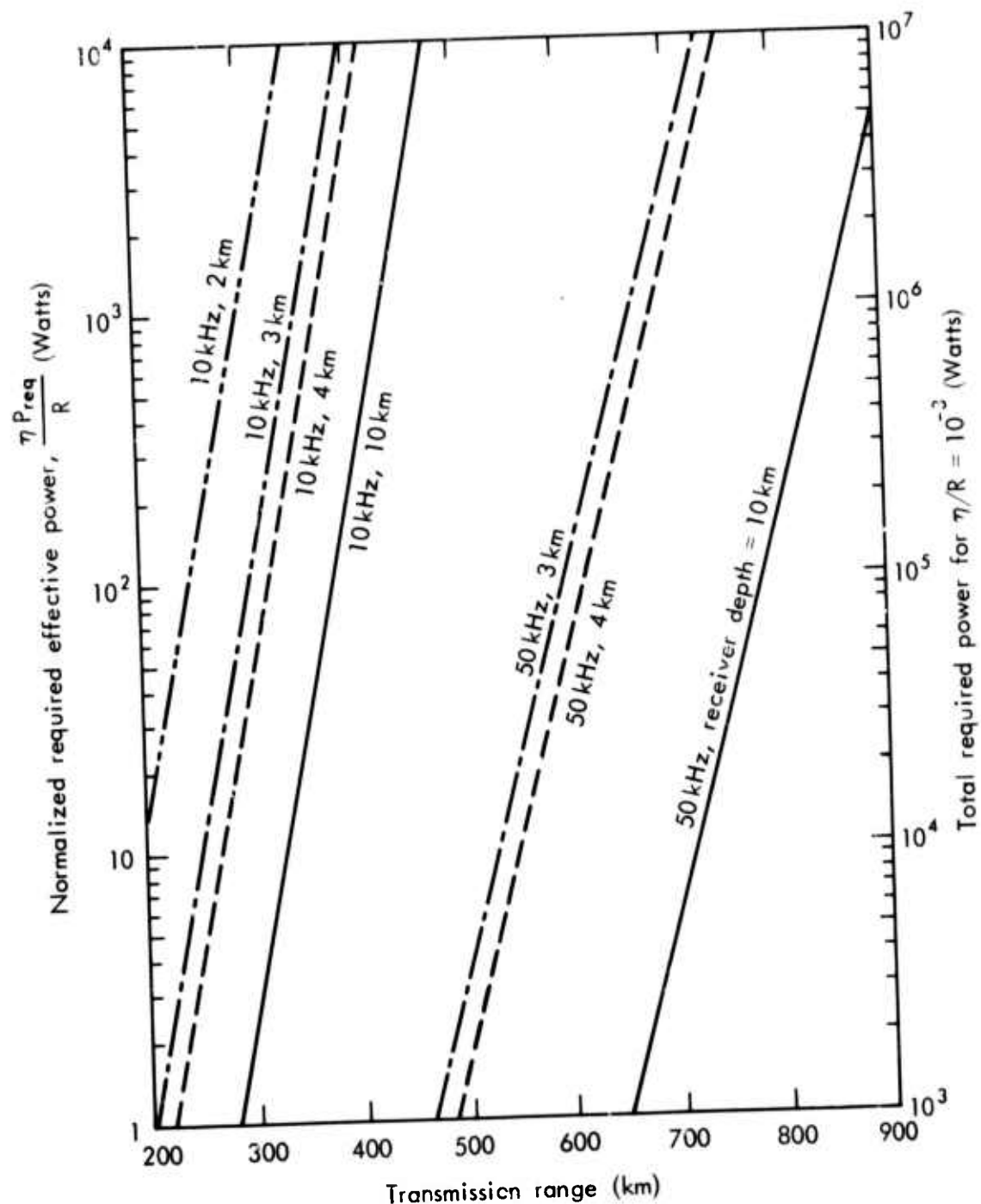
Fig. 17--Transmission Range vs. Effective Power and Total Power
for Several Receiver Depths (Keller Profile)

become *so* large that the corresponding reduction in transmission range would probably be intolerable. Note also that for lower frequencies (e.g., 10 kHz or less--see Fig. 15), the fractional degradation in transmission range incurred by using shallow receiver depths is less severe than at 50 kHz. Nonetheless, for depths greater than about three kilometers, the higher frequencies are still preferable.

Figure 18 is completely analogous to Fig. 17 except that it applies to the Housley BR (assumed transition at 25 km) model. Should this model prove to be a reasonably good representation of crustal conductivities over large geographic regions, then transmission ranges approaching 5000 km could be achievable for receivers placed at depths of about ten kilometers. Even for receiver depths as shallow as 3 or 4 km, ranges in excess of 3000 km are a possibility. Again, frequencies of several tens of kilohertz are preferable to lower frequencies. Detailed results have not been shown for the Housley EUS model. The achievable transmission ranges based on this model would be of the order of 10,000 km.

We have not explicitly considered situations for which the lithospheric conductivity profile exhibits lateral variations over the propagation path. Of course such variations would be expected to occur in situations of practical interest; e.g., propagation between two geological provinces.[*] Mode conversion caused by lateral variations is not expected to be large enough to alter the main conclusion of this study (*Wait and Spies, 1972*). Thus, the transmission through a

---

[*] For a discussion of evidence that good lateral continuity *does* exist over large distances, see *Heacock (1971)*, pp. 1-9.
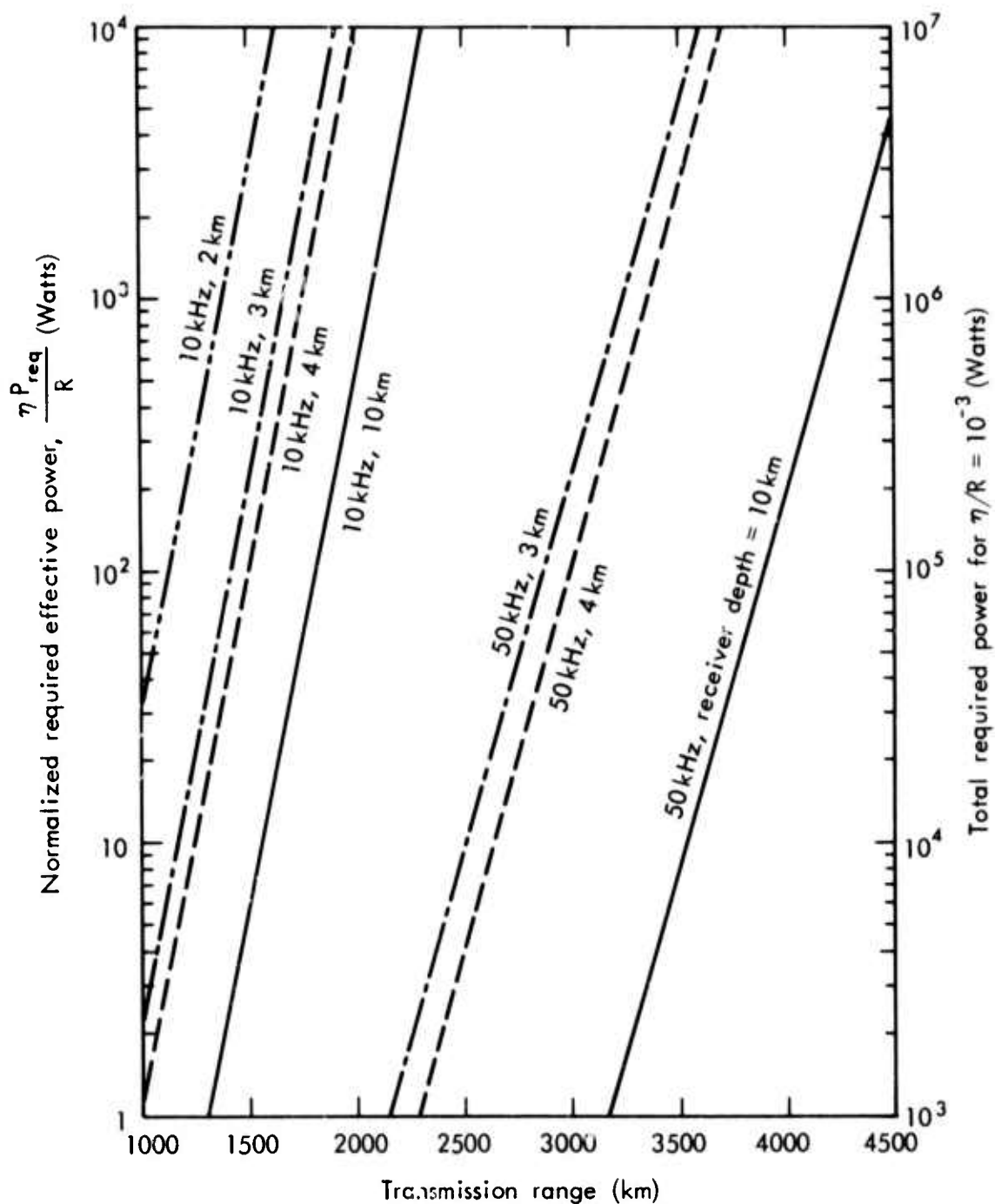
Fig. 18--Transmission Range vs. Effective and Total Power for
Several Receiver Depths (Housley BR Profile)

non-stratified lithosphere can be estimated reasonably well by simply summing the attenuation suffered in each region, using the appropriate attenuation rates (Fig. 6, p. 34) and path lengths. The depth-degradation factor, however, depends solely on the properties of the lithosphere in the vicinity of the receiver.

The existence, or non-existence, of sharp transitions in conductivity on the bottomside of the waveguide can alter the maximum transmission range by about a factor of two. An example of this effect is given in Fig. 19, which shows the degradation in calculated transmission range that occurs as the depth of the assumed lower reflecting layer in the Housley BR model is increased beyond 25 km. Of course, *improvements* would occur for shallower layer depths, as they would if either the Housley EUS or SN profiles were used (Fig. 3, p. 13). Clearly, field experiments (see *Hales, 1972; Keller, 1972*), as well as studies of the relation of laboratory data to *in situ* rocks, must be undertaken if these uncertainties are to be satisfactorily resolved.

In regions where the conductivity profile at depths shallower than 8 km is similar to that shown by Keller (Fig. 2, p. 10) rather than as shown by Levin (Fig. 1, p. 9), antenna burial depths of only 3 or 4 km should be adequate for a meaningful propagation experiment. As indicated by the results shown in Fig. 17, other conditions would also have to be satisfied:

1) Combinations of transmitter efficiency, bandwidth (R), and total power should be selected so that the power *radiated* into the lowest TM mode is at least a few watts. (The corresponding requirement for total power could be well in excess of a kilowatt.)
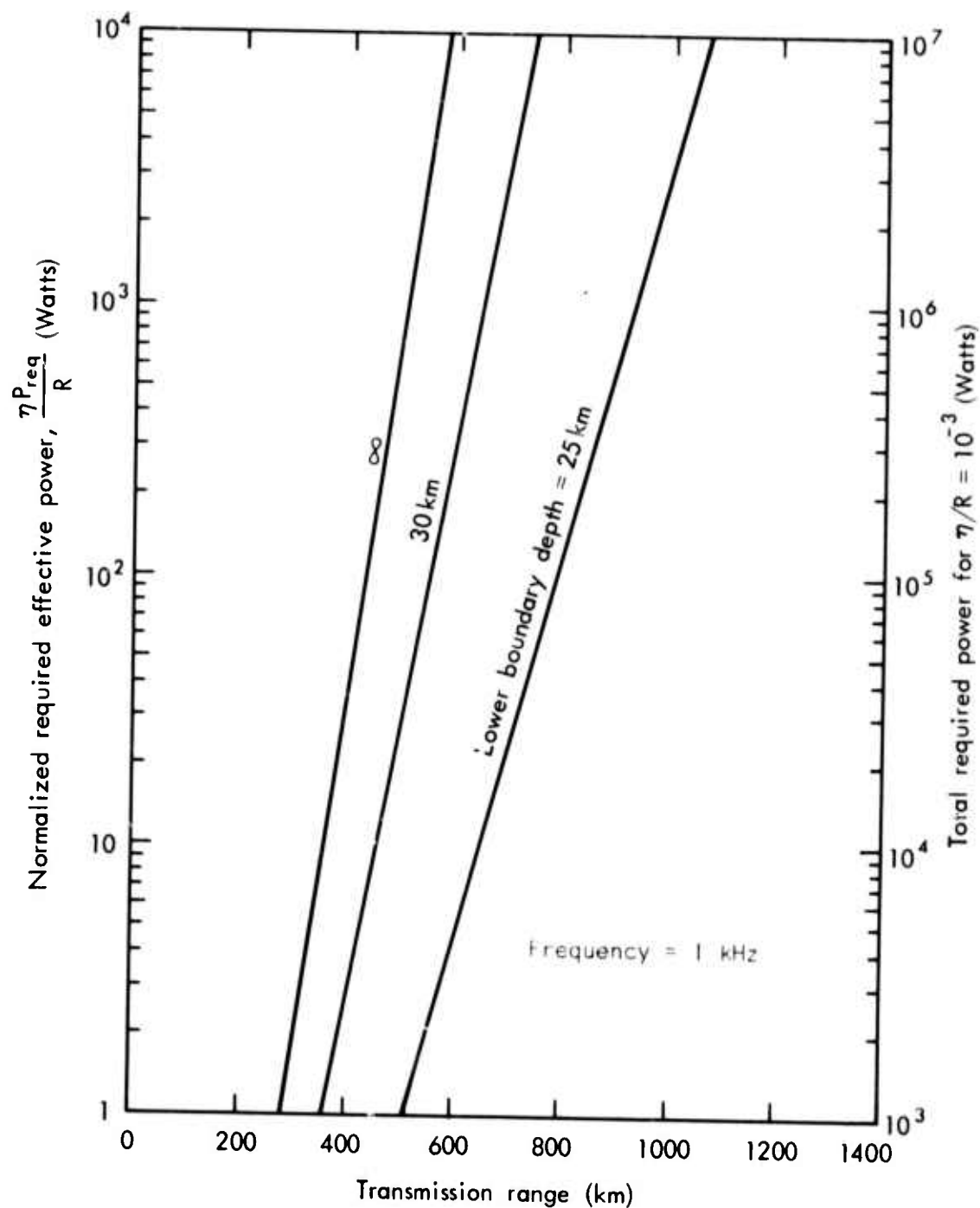
Fig. 19--Transmission Range vs. Effective and Total Power for
Several Depths of Assumed Sharp Transition in Conductivity
(Housely BR Profile, 10-km Receiver Depth)

2) A frequency of several tens of kilohertz should be used.

As discussed by *Levin (1971)*, a propagation experiment has been carried

out at a frequency of 2.2 kHz, a total power of 2.5 kilowatts, and with

3-km deep boreholes. The negative outcome of this experiment does not

provide conclusive evidence that favorable conductivity profiles are non-

existent in nature. The 2.2 kHz frequency was much lower than optimum,

and the antenna efficiency might well have been too poor to provide

adequate REP from the 2.5-kilowatt total power. Further, the 3-km deep

boreholes may simply have been too shallow for the particular region

where the experiment was carried out--deeper boreholes or a different

test site being needed. Clearly, very careful site selection and antenna

design are needed for a conclusive experiment.

REFERENCES

Blackwell, D. D., "The Thermal Structure of the Continental Crust," *The Structure and Physical Properties of the Earth's Crust,* J. G. Heacock, ed., AGU Monograph 14, 1971.

Brace, W. F., "Resistivity of Saturated Crustal Rocks to 40 km Based on Laboratory Studies," *The Structure and Physical Properties of the Earth's Crust,* J. G. Heacock, ed., AGU Monograph 14, 1971.

Budden, K. G., *The Waveguide Mode Theory of Wave Propagation,* Logos Press, London, 1961.

Evans, J. E., and A. S. Griffiths, "Design of an ELF Noise Processor," *Engineering in the Ocean Environment,* IEEE Publication 72 CHO 660-1 OCC, 1972.

Field, E. C., "The Effects of Ions on Very-Low-Frequency Propagation during Polar Cap Absorption Events," *Radio Science, Vol. 5,* 1970.

Gallawa, R. L., and L. L. Haidle, *An Engineering Feasibility Study of Communications via a Subterranean Waveguide,* Institute for Tele-communication Sciences, OT/TRER 39, November 1972.

Hales, A. L., *et al., A Multidisciplinary Program of Investigation of the Possibility of an Electromagnetic Wave Guide in the Lower Crust,* University of Texas at Dallas (March 7, 1972).

Heacock, J. G., ed., *The Structure and Physical Properties of the Earth's Crust,* AGU Monograph 14, 1971.

Housley, R. M., private communication, 1973; also, Simmons, G., R. M. Housley, and F. J. Forin, "Electrical Resistivity of Rocks and the Possibility of Lithospheric Communication," to be published, 1973.

Keller, G. V., "Electrical Studies of the Crust and Upper Mantle," *The Structure and Physical Properties of the Earth's Crust,* J. G. Heacock, ed., AGU Monograph 14, 1971.

Keller, G. V., *et al., Recommendation of the Working Group on Electromagnetic Methods* (March 6, 1972).

Keller, G. V., private communication, 1973.

Levin, S. G., "Radio Propagation through the Crust-Retrospect and Prospect," *The Structure and Physical Properties of the Earth's Crust,* J. G. Heacock, ed., AGU Monograph 14, 1971.

Maxwell, E. L., "Atmospheric Noise from 20 Hz to 30 kHz," *Radio Science, Vol. 2,* June 1967.

Spies, K. P., and J. R. Wait, *On Calculations of the Modal Parameters of an Idealized Earth-Crust Waveguide*, Institute for Telecommunication Sciences, Tech. Rept. N. 1, March 17, 1971.

Wait, J. R., "An Anomalous Propagation of Radio Waves in Earth Strata," *Geophysics, 19(2)*, 1954.

Wait, J. R., and K. P. Spies, *On Mode Conversion in the Earth-Crust Waveguide*, Inst. for Telecommunication Sciences, Tech. Rept. No. 4, 27 October 1972.

Wheeler, H. A., "Radio Wave Propagation in the Earth's Crust," *Radio Sci., 65D(2)*, 1961.

DOCUMENT CONTROL DATA - R & D

(Security classification of title, body of abstract and indexing annotation must be entered when the overall report is classified)

1. ORIGINATING ACTIVITY (Corporate author)	2a. REPORT SECURITY CLASSIFICATION
Pacific-Sierra Research Corporation 1456 Cloverfield Blvd. Santa Monica, California 90404	Unclassified
	2b. GROUP NA

3. REPORT TITLE

ELECTORMAGNETIC COMMUNICATION IN THE EARTH'S CRUST

4. DESCRIPTIVE NOTES *(Type of report and inclusive dates)*

Semiannual Technical Report

5. AUTHOR(S) *(First name, middle initial, last name)*

Edward C. Field and Michael Dore

6. REPORT DATE	7a. TOTAL NO. OF PAGES	7b. NO. OF REFS
June 29, 1973	72	18

8a. CONTRACT OR GRANT NO.	9a. ORIGINATOR'S REPORT NUMBER(S)
N00014-73-C-0189	
b. PROJECT NO. ARPA Order No. 2270/8-16-72	PSR Report 306
c. Program Code No. 3F10	9b. OTHER REPORT NO(S) *(Any other numbers that may be assigned this report)*
d.	

10. DISTRIBUTION STATEMENT

Each transmittal of this document outside the agencies of the U.S.
Government must have prior approval of Code 417, Office of Naval Research.

11. SUPPLEMENTARY NOTES	12. SPONSORING MILITARY ACTIVITY
	Advanced Research Projects Agency 1400 Wilson Blvd. Arlington, Virginia 22209

13. ABSTRACT

This report presents results of an analysis of the capabilities that might be achieved with a lithospheric communication system. The analysis uses several available models of continental lithospheric conductivity as inputs to calculations of transmission characteristics and possible communication system parameters. Because of prevailing uncertainties, significant differences exist among the various models; and a wide range of future system capabilities is found to lie within the realm of possibility.

For all models used, the calculated attenuation rates are considerably larger than for above-ground transmission, which depends on propagation in the earth-ionosphere waveguide. In spite of this fact, reasonably large transmission ranges might be possible in the lithosphere because the atmospheric noise fields at depth are very small, having suffered heavy attenuation in propagating downward from the earth's surface.

The major factor affecting system feasibility is whether water-saturated microcracks exist in all major rock types at depths greater than, say, 5-to-8 km. If such microcracks exist (as assumed in one model), and minimum conductivities in the crust exceed $10^{-5} - 10^{-6}$ mhos/m, then the calculations show clearly that a practical communication system is not feasible. For this case, the attenuation rates are so high that only very short transmission ranges could be achieved, even if large amounts of power were expended. Field experiments will be needed to determine with certainty whether saturated microcracks are, in fact, present at the depths of interest.

SEE ATTACHED PAGE

1 4	KEY WOROS	LINK A		LINK B		LINK C	
		ROLE	WT	ROLE	WT	ROLE	WT
	lithosphere						
	communications						
	military communications						
	very-low-frequency propagation						

CONTINUATION OF ABSTRACT

However, valid reasons exist for optimism that fluids (or fluid films) should not be an important factor at depths greater than several kilometers, and that conductivity profiles (at depth) based on laboratory data for dry rocks more closely approximate actual conditions. Further, recent laboratory data indicate that the conductivity of dry rock in the crust could be much lower (10^{-8} to 10^{-9} mhos/m) than previously believed (10^{-7} mhos/m). It is, of course, difficult to relate data obtained from laboratory samples to conductivities of rock *in situ*. Nonetheless, calculations using conceptual profiles based on the assumption of dry basement rock yield results that are quite encouraging. For example, for data rates of a few tens of bits-per-second and power expenditures of 1-to-10 megawatts, transmission ranges of from about 1000 to many thousands of kilometers (depending on the profile used) appear to be a possibility.

The calculations show clearly that much larger transmission ranges can be achieved in the LF band (30-100 kHz) than at the lower frequencies considered. This effect is due mainly to the heavy attenuation suffered by downward propagating atmospheric noise at the higher frequencies. The calculations also show that the maximum transmission ranges are somewhat sensitive to the details of the model profiles. For example, for two profiles exhibiting the same minimum conductivity, the transmission range (for a specified power, etc.) can vary by a factor of two depending on the conductivity depth-gradients, and the precise location of any sharp transition layers that might exist.

The depth to which a receiver must be buried to achieve satisfactory performance is a particularly important parameter, since borehole drilling costs could be a large fraction of the total system cost. The transmission ranges given above apply when the receiving antenna is located near the "center" of the waveguide--assumed to be about ten kilometers deep for the conductivity profiles used in this report. For profiles representative of regions stripped of highly conductive sedimentary layers, the calculations show that receiver depths as shallow as 3 or 4 km could be used at only a 15-to-20 percent penalty in transmission range.

DISTRIBUTION LIST

Director   2 copies
Advanced Research Projects Agency
1400 Wilson Boulevard
Arlington, Virginia 22209
Attention: Program Management

Defense Documentation Center   12 copies
Cameron Station
Alexandria, Virginia 22314

STO1AC   1 copy
Battelle Memorial Institute
505 King Avenue
Columbus, Ohio 43201

Office of Naval Research   3 copies
800 North Quincy Street
Arlington, Virginia 22217
Attention: Code 417

Office of Naval Research   1 copy
1030 E. Green Street
Pasadena, California 91106

Commander, Defense Contract Administrative   1 copy
    Services District, Los Angeles
11099 So. La Cienega Blvd.
Los Angeles, California 90045
Attention: DCRL-DLCB-C4

Director   6 copies
Naval Research Laboratory
Washington, D.C. 20390
Attention: Code 2629

Director   6 copies
Naval Research Laboratory
Washington, D.C. 20390
Attention: Code 2627

Office of Naval Research
800 North Quincy Street
Arlington, Virginia 22217
Attention: Dr. Sidney G. Reed, Jr., Code 102T
             Dr. Thomas P. Quinn, Code 418
             Dr. Robert G. Morris, Code 421

Director
Naval Research Laboratory
Washington, D.C. 20390
Attention: Mr. William E. Garner, Code 5460
             Dr. John Davis, Code 5464
             Dr. L. B. Wetzel, Code 5400

Defense Communication Agency
8th and S. Courthouse Road
Arlington, Virginia 20390
Attention: Capt. Richard S. Gardiner, Code 960

Dr. Samuel Koslov, OASN (R&D)
Room 4E741
Pentagon Building
Washington, D.C. 20350

Chief Scientist, Code OP094H
Command Support Programs
Room 4C558
The Pentagon
Washington, D.C. 20350

Naval Electronic Systems Command
Special Communications Project Office
National Center #1
Arlington, Virginia 20360
Attention: Mr. John E. Doncarlos, PME 117T

Deputy Assistant Secretary (Systems) OSD(T)
Room 3D174 - The Pentagon
Washington, D.C. 20350
Attention: Dr. Howard L. Yudkin

Deputy Director Strategic Submarine
Command and Control Program Office
Room 5D584 - The Pentagon
Washington, D.C. 20350
Attention: Capt. William H. Lynch, Code OP094RB

Foreign Technology Division
Wright-Patterson Air Force Base
Dayton, Ohio 44223
Attention: Capt. John D. Mill (USAF)

Mr. Edward J. Kolb
Naval Security Station
3801 Nebraska Avenue, N.W.
Washington, D.C. 20390

Mr. Clarence Sargent
Room 4G04
CIA Headquarters
Washington, D.C. 20505

U.S. Army Electronic Command Headquarters
Ft. Monmouth, New Jersey 07703
Attention: Mr. Morris Acker

Mr. Finn Bronner
Army Research Office
Durham, North Carolina

Dr. James R. Wait
Environmental Research Labatories
U.S. Department of Commerce
Room 231, Research Building #1
Boulder, Colorado 80302

Dr. Robert L. Gallawa
Office of Telecommunications
Institute for Telecommunication Sciences
U.S. Department of Commerce
Boulder, Colorado 80302

Dr. D. D. Crombie
Associate Director
Institute for Telecommunication Sciences
U.S. Department of Commerce
Boulder, Colorado 80302

Mr. Frank Finlan
Ordnance Research Laboratory
Pennsylvania State University
State College, Pennsylvania 16802

Commander H. E. Sprecher, Jr., Code 543
Naval Ordnance Systems Command
National Center #2
2521 Jefferson Davis Highway
Arlington, Virginia 20360

Professor Charles S. Cox
Scripps Institution of Oceanography
University of California
La Jolla, California 92037

Professor Gene M. Simmons
Department of Earth and Planetary Sciences
Massachusetts Institute of Technology
Bldg. 54-314
Cambridge, Massachusetts 02139

Professor George V. Keller
Colorado School of Mines
Golden, Colorado 80401

Dr. Robert M. Housley
Science Center Rockwell International
Planetary Physics
P.O. Box 1085
1049 Camino Dos Rios
Thousand Oaks, California 91360

Professor Stanely H. Ward
Department of Geological & Geophysical Sciences
University of Utah
Salt Lake City, Utah 84112

Geomagnetics and Electrical Geoscience Research
  Laboratory
Engineering-Science Bldg. 623
Austin, Texas 78712
Attention: Professor H. W. Smith
             Professor F. X. Bostick

Professor R. B. Smith
University of Utah
Department of Geological & Geophysical Sciences
Salt Lake City, Utah 84112

Professor Mark Landisman
Geosciences Division
University of Texas
P.O. Box 30365
Dallas, Texas 75230

Mr. Robert A. Moore
Office of Defense Research & Engineering
Room 3E129
The Pentagon
Washington, D.C. 20030

Mr. P. Haas
Defense Nuclear Agency
Washington, D.C. 20305

Mr. D. Evelyn
Defense Nuclear Agency
Washington, D.C. 20305

Mr. W. Heilig
Defense Communications Agency
Washington, D.C. 20305

Dr. W. A. Decker
P.O. Box 1925
Main Station
Washington, D.C. 20013

Defense Intelligence Agency
Washington, D.C. 20301
Attention: DIADT

Dr. B. Krueger
Naval Electronics Systems Command
Department of the Navy
Washington, D.C. 20360

Mr. Dan Barney
Code 53212
Naval Intelligence Systems Command
1136 Hoffman Building
Alexandria, Virginia 22314

Mr. Jerry Batts (NISC-42)
Naval Intelligence Support Center
3201 Suitland Road
Washington, D.C. 20390

Dr. E. Lewis
Air Force Cambridge Research Laboratory
L.G. Hanscom Field
Bedford, Massachusetts 01730

Colonel E. C. Mixon
DCS/Research & Development
Headquarters, USAF (AFRDQ)
Washington, D.C. 20330

Mr. T. Kamm
Air Force Weapons Laboratory
Kirtland Air Force Base,
New Mexico 87117

Dr. Robert Jones
Foreign Science & Technology Center
Charlottsville, Virginia 22901

Dr. A. M. Peterson
Stanford Research Institute
333 Ravenswood Avenue
Menlo Park, California 94025

Dr. A. Fraser-Smith
Stanford University
Stanford, California 94305

Dr. C. Greifinger
Research & Development Associates
525 Wilshire Blvd.
Santa Monica, California 90403

Mr. D. H. Blumberg
Computer Science Corporation
1095 Duane Court, Suite 211
Sunnyvale, California 94086

Mr. M. D. White
Massachusetts Institute of Technology
Lincoln Laboratory
P.O. Box 73
Lexington, Massachusetts 02173

Mr. Mario Grossi
Raytheon Company
528 Boston Post Road
Sudbury, Maryland 01776

Dr. K. Powers
Research Corporation of America
301 Ridgeview Road
Princeton, New Jersey 08540